Cosmic ray detection in space

Valerio Vagelli
I.N.F.N. Perugia, Università degli Studi di Perugia
Corso di Fisica dei Raggi Cosmici A.A. 2018/2019

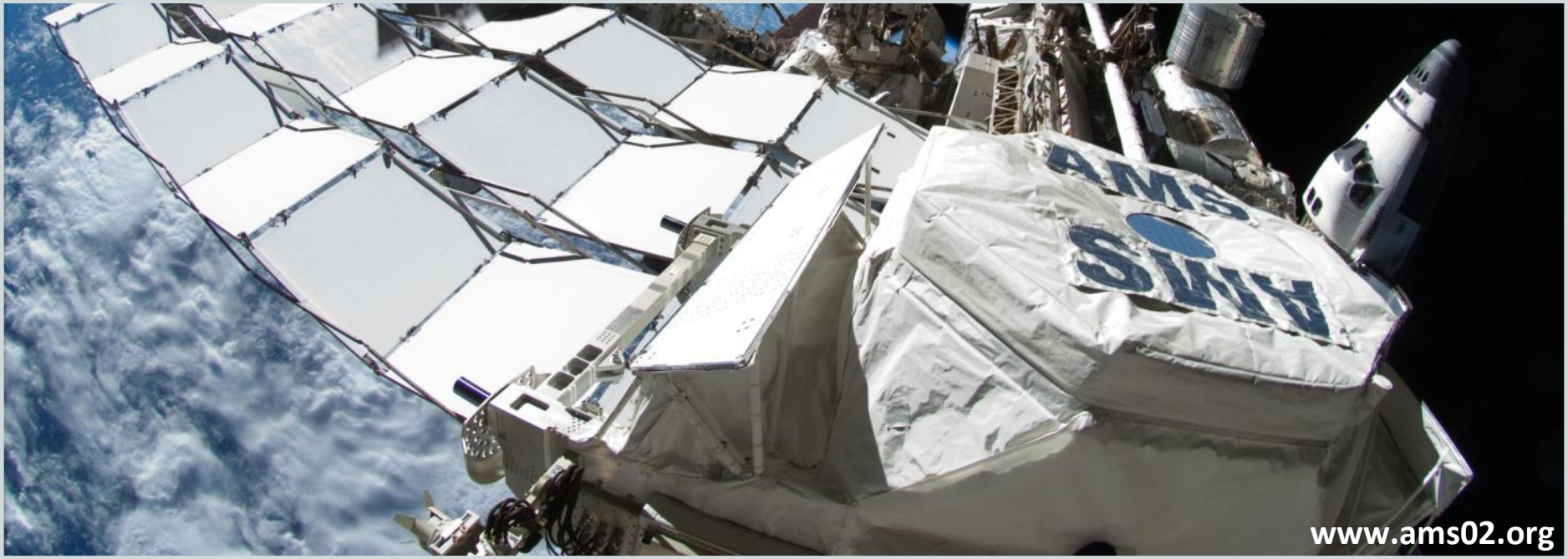

i) Introduction to Cosmic Rays
ii) Space Borne Experiments
iii) The AMS-02 detector

Valerio Vagelli
I.N.F.N. Perugia, Università degli Studi di Perugia
Corso di Fisica dei Raggi Cosmici A.A. 2018/2019

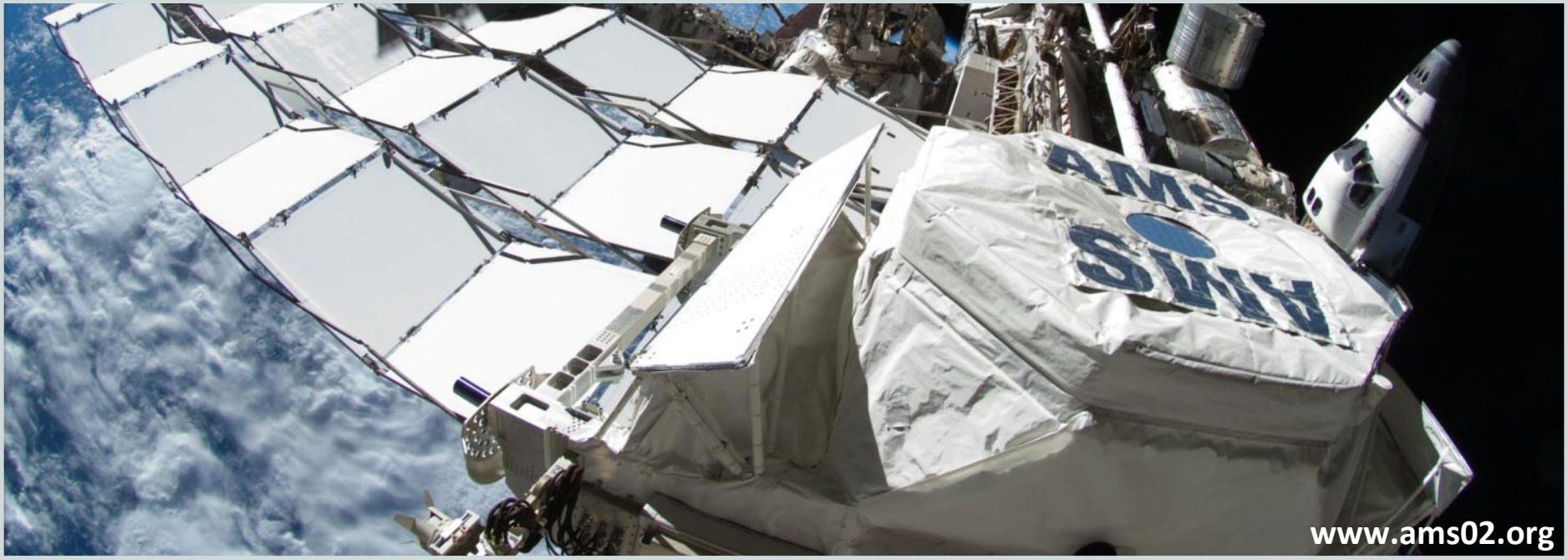

Cosmic Rays

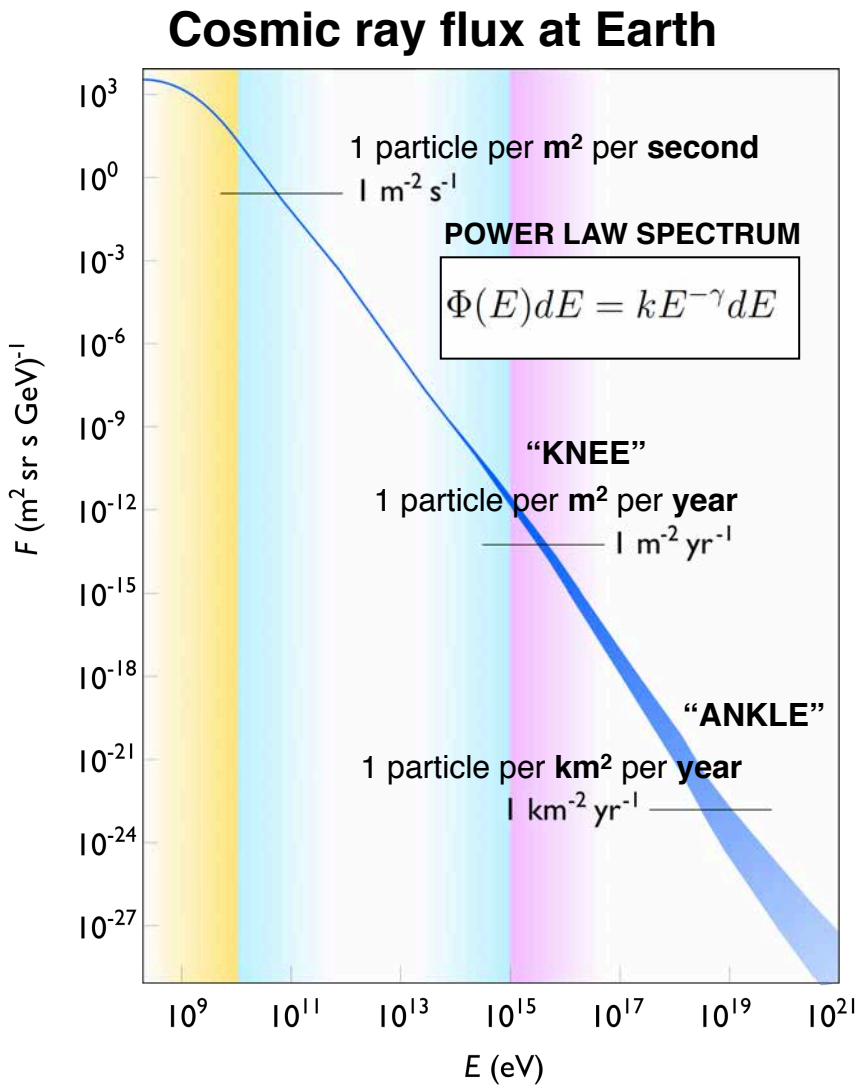

- Cosmic ray Flux: Intensity of CR in space per **unit of area, solid angle, time and energy**
- Energy range up to **10^{20} eV**
- Intensities spanning **30 orders of magnitude**
- Most of cosmic rays are **protons and nuclei**

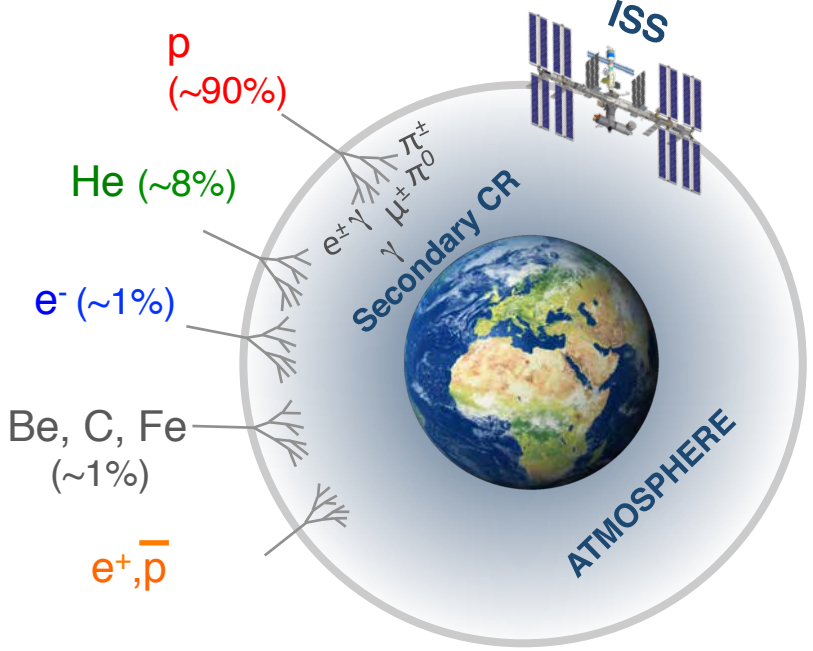

Experimental detection

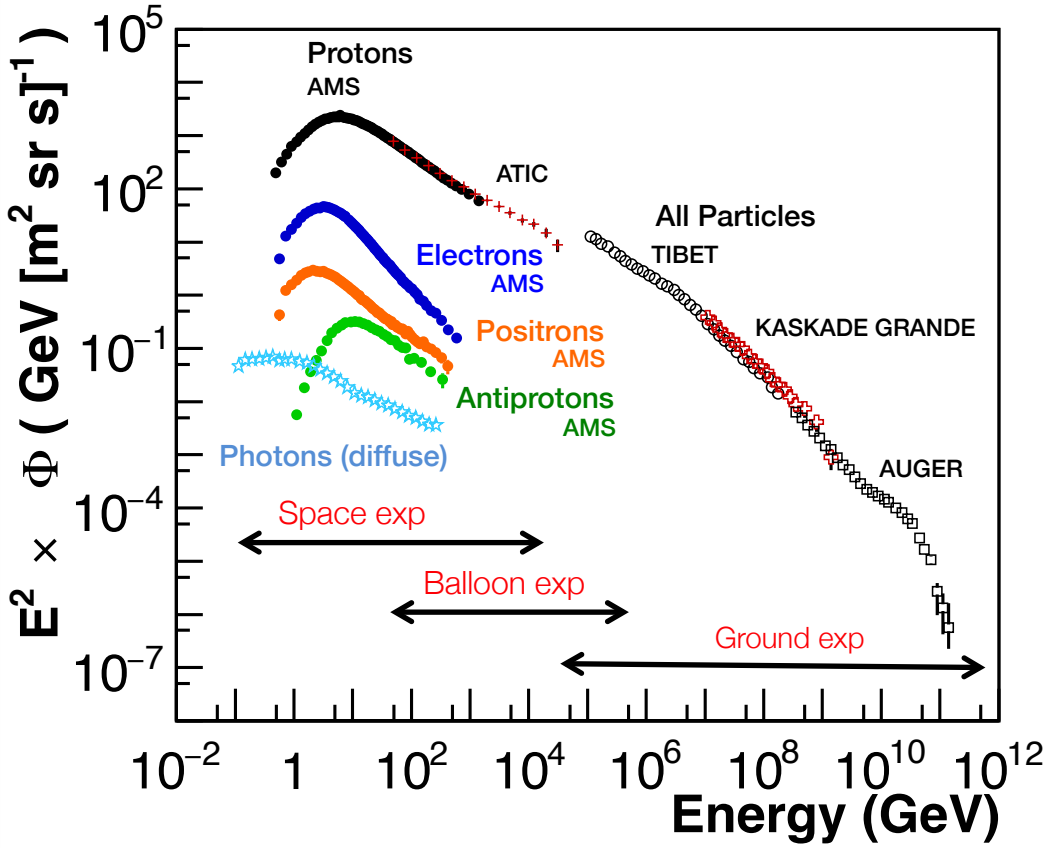

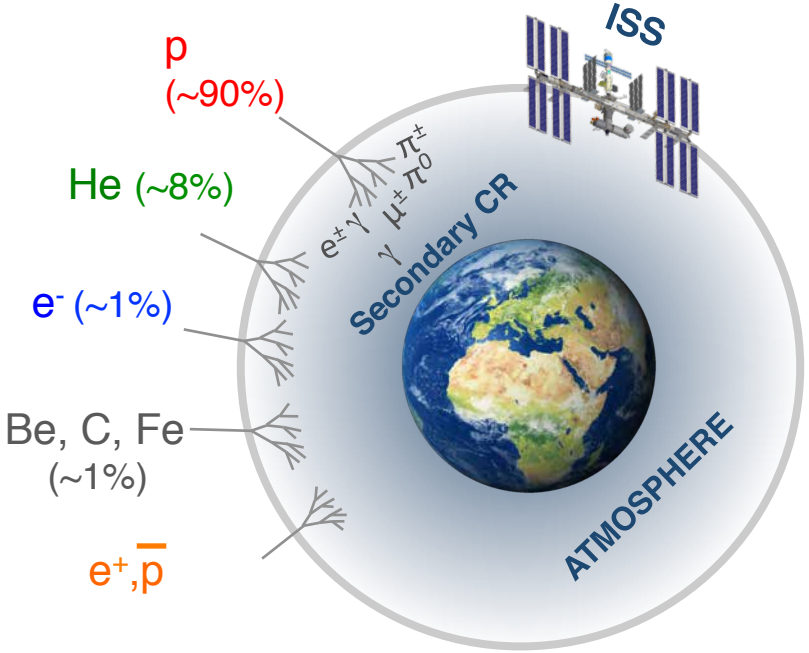

- Primary cosmic rays interact with atmosphere. Only secondary CRs from interactions reach the ground.
- Flux steeply falling as function of energy. Need large collection areas

Ground based experiments

Charged CRs

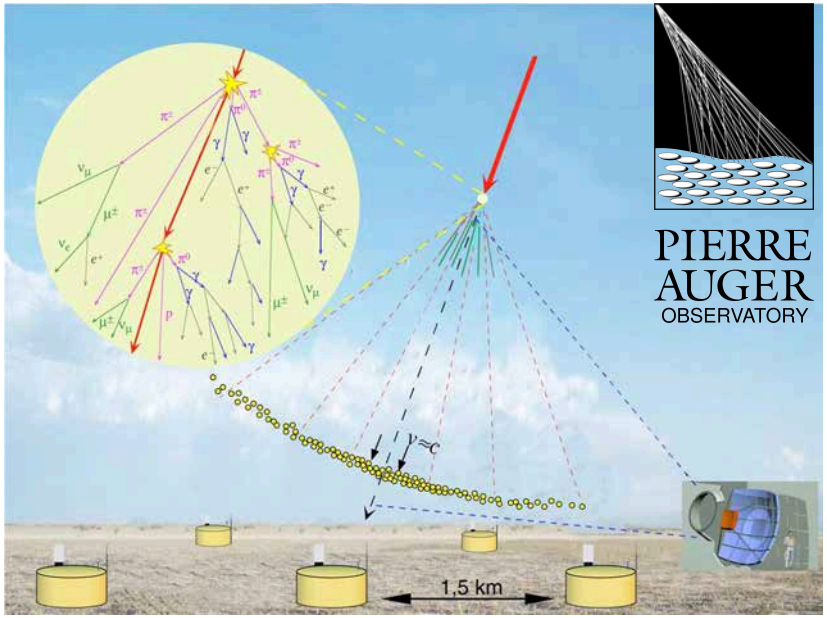

Gamma Rays

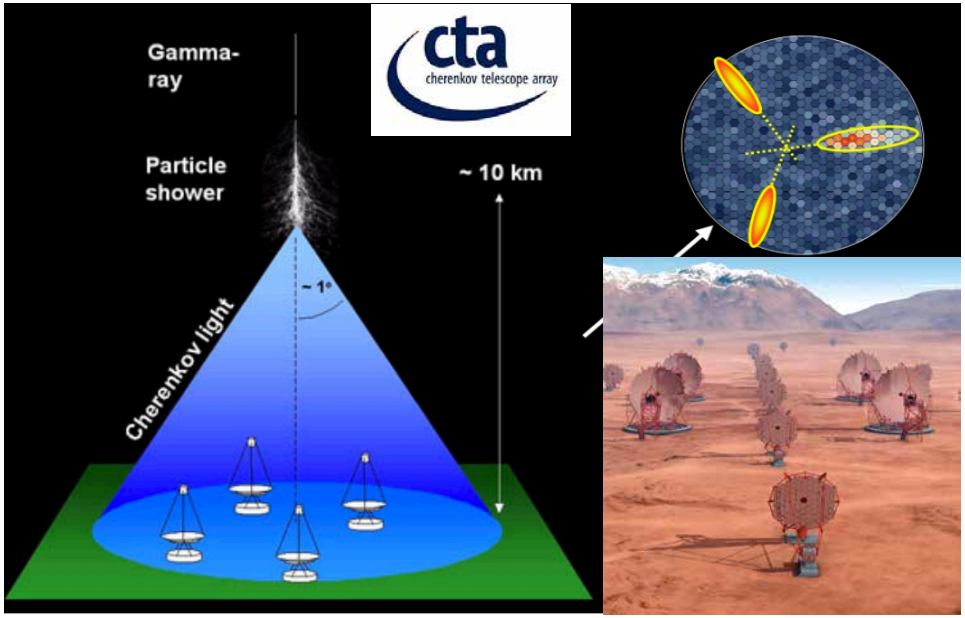

- √ Large collection areas → probe CR energies TeV –Eev ranges
- X Indirect measurements
  - Primary CR identified via the analysis of shower shapes and composition at ground (highly rely on MonteCarlo simulations)
  - Main systematics are the parametrization of X-sections at very high energies

Balloon experiments

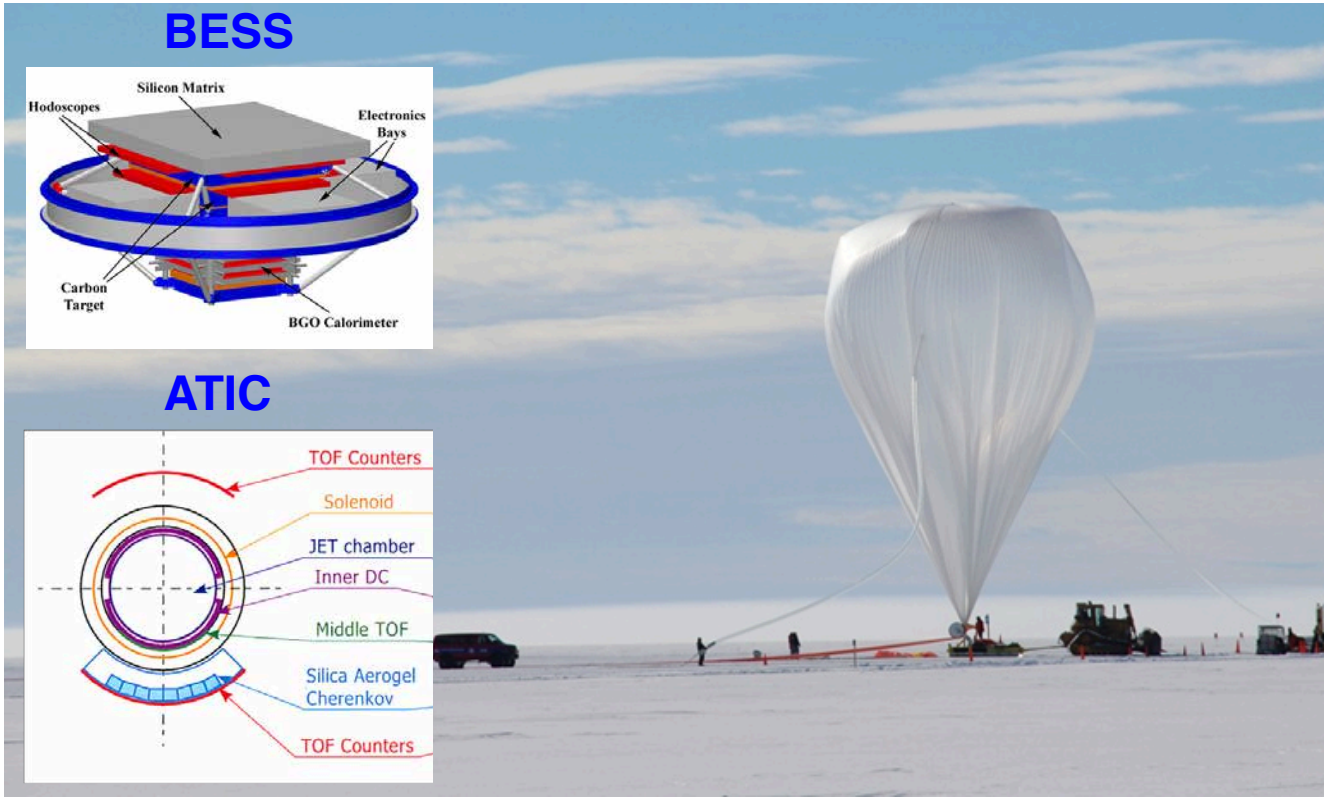

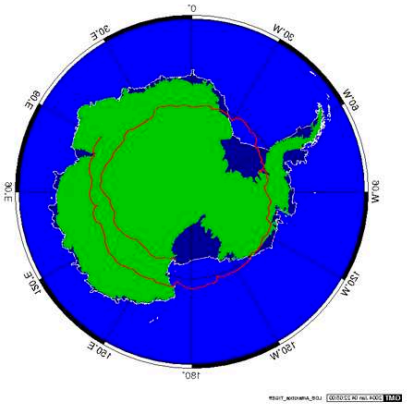

- √ Larger acceptances than space borne experiments
- √ Direct measurements
- X Orbit limited at North poles for maximum 1 month
- X Residual atmosphere above the payload

Space Borne experiments

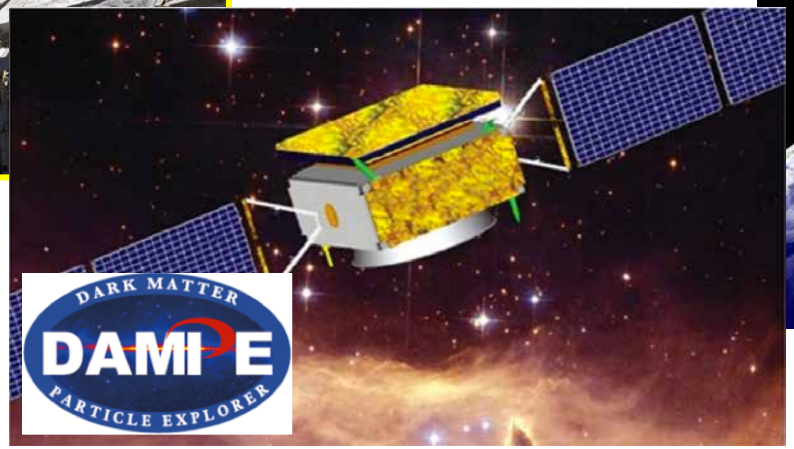

- √ Direct measurements outside atmosphere
- √ Continuous duty cycles, typically many years of lifetime
- √ Field of view covering the whole sky
- X Smaller acceptances
- X Operation in space and communications not trivial
- X “Use once and destroy”

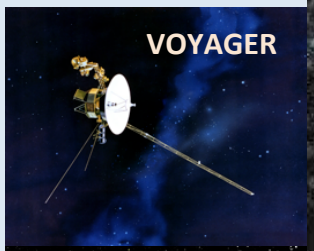

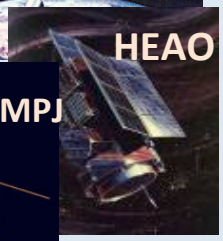

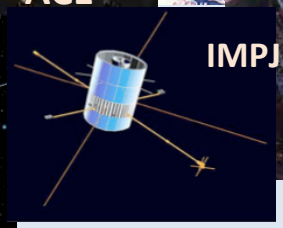

Long missions (years)
Small payloads
Low energies..

IMP series < GeV/n
ACE-CRIS/SIS Ekin < GeV/n
VOYAGER-HET/CRS < 100 MeV/n
ULYSSES-HET (nuclei) < 100 MeV/n
ULYSSES-KET (electrons) < 10 GeV
CRRES/ONR < (nuclei) 600 MeV/n
HEAO3-C2 (nuclei) < 40 GeV/n

Short missions (days)/ Larger payloads

CRN on Challenger
(3.5 days 1985)

AMS-01 on Discovery
(8 days, 1998)

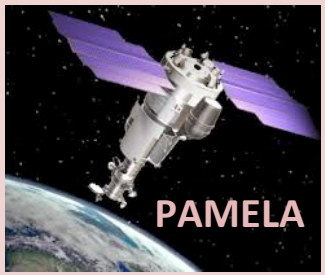

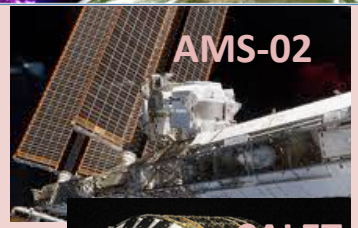

Long missions
Large payloads

Operations in Space

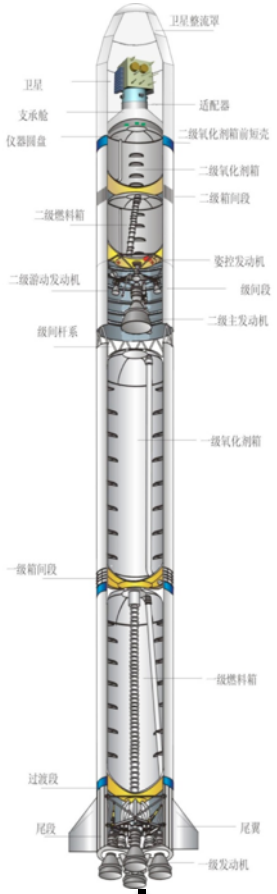

Mechanical stress at launch:
- **Static acceleration**
- **Random vibration**
- **Sinusoidal vibration**
- **Pyroshock**

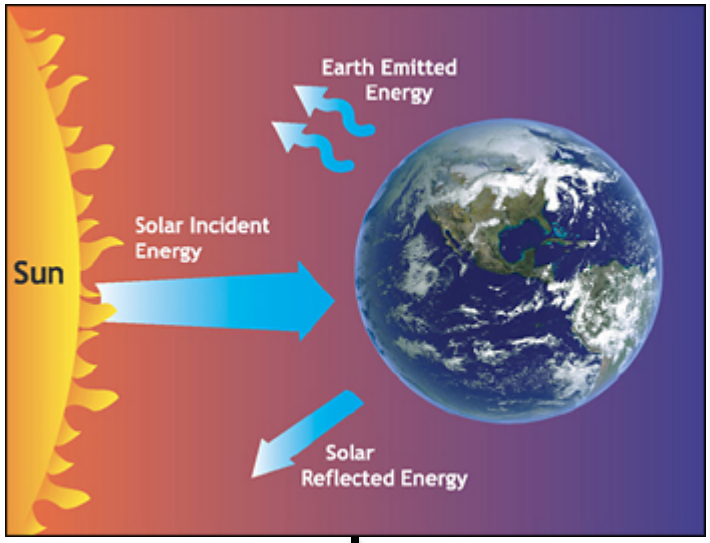

Life in space:
- **Thermal stresses due to Sun-light (seasonal / day-night effects)**
- **Vacuum**

Careful Design, Model validation and Qualification are needed to ensure *highest possible reliability*

Operations in Space

Space is a harsh environment

Full space qualification sequence before launch:

- Operational tests after stress
- Verification of dynamical behaviour
- Verification of thermal model

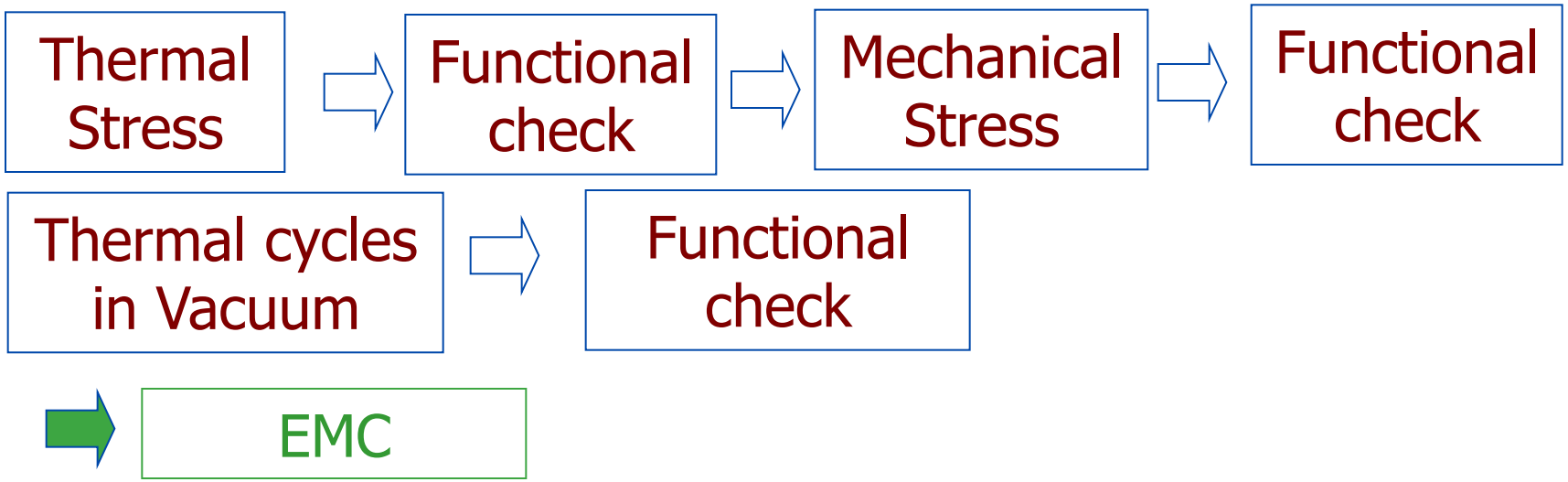

Operations in Space

Space is a harsh environment

Typically 3 step for test procedure:
Thermal, Vibration, Thermo-Vacuum

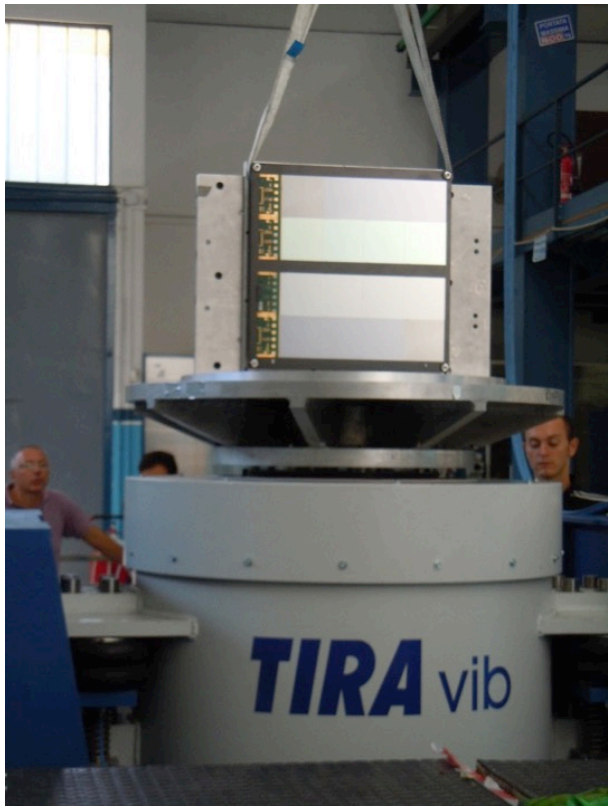

Operations in Space

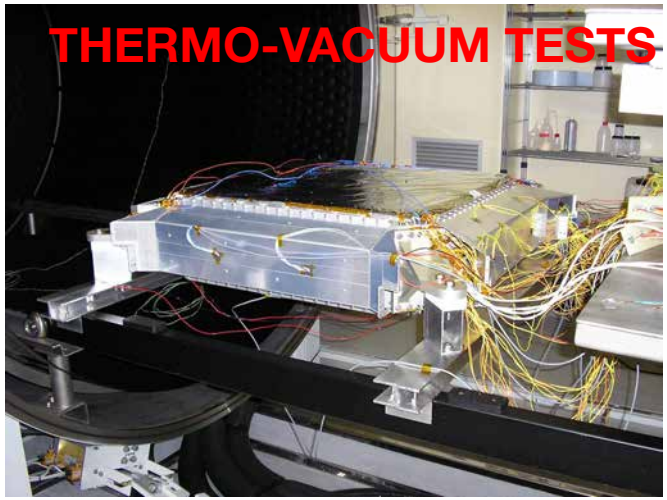

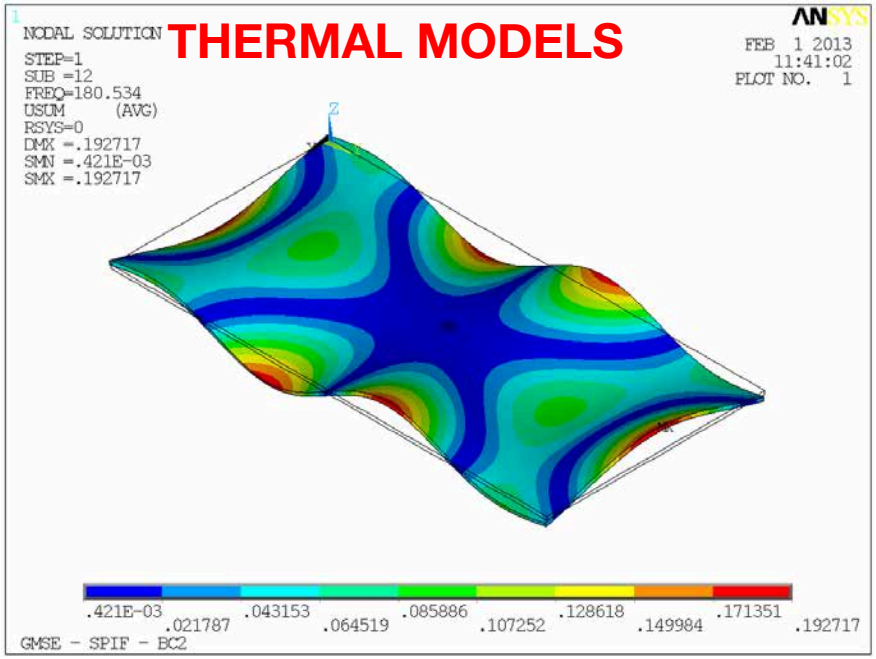

The long process to fly….

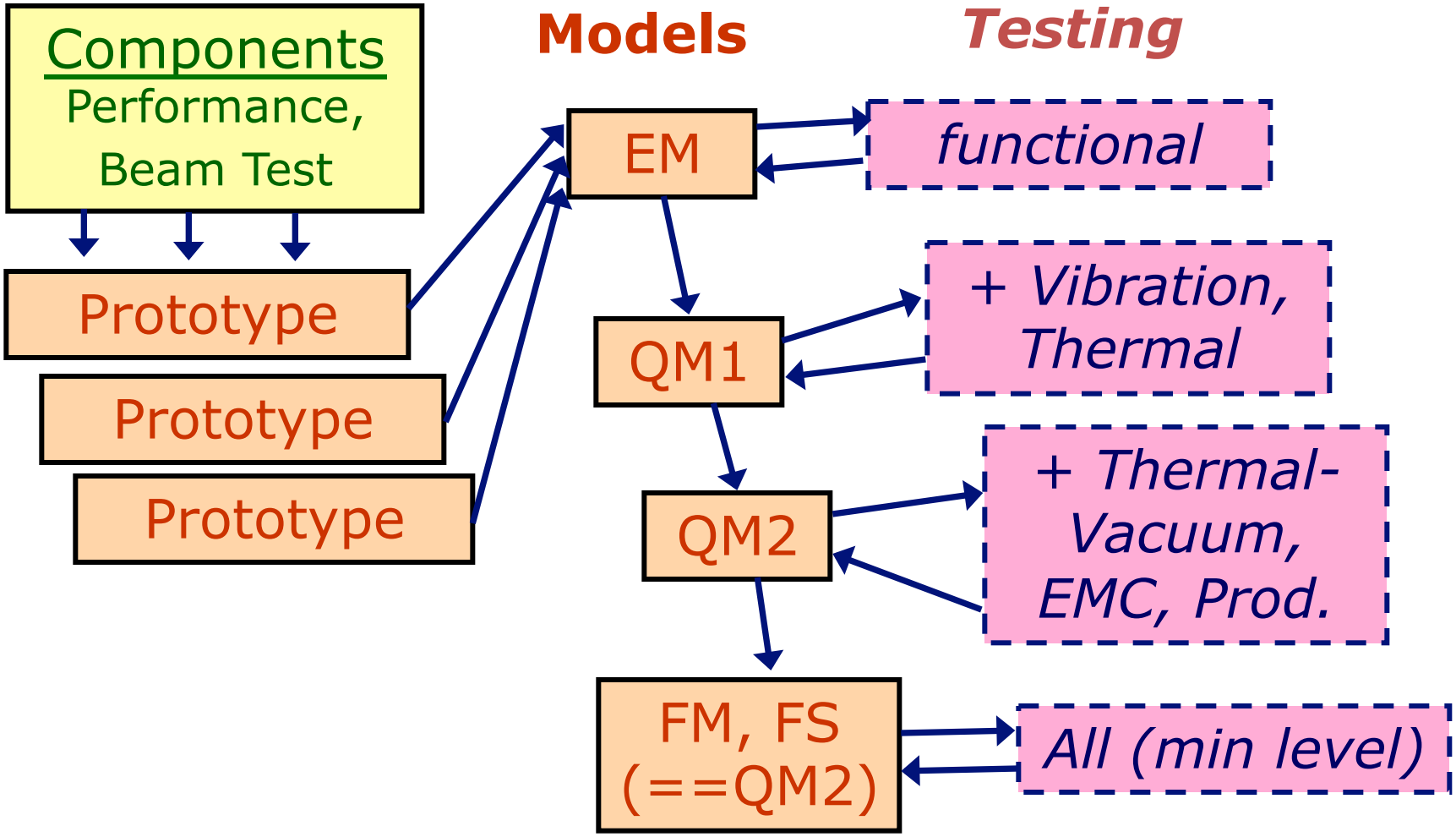

Particle Identification (in space)

- Direct identification of the cosmic rays via measurement of their
  - **Velocity** (Time of Flight systems, Cherenkov Radiation detectors)
  - **Charge** (dE/dX detectors, Cherenkov Radiation detectors)
  - **Energy or Rigidity** (Calorimeters, Spectrometers)
  - **Sign of the charge** (Spectrometers)
  - **Peculiar Interactions** (TR detectors, Calorimeters, Neutron detectors, …)
  - **Incoming Direction** (Tracking detectors)

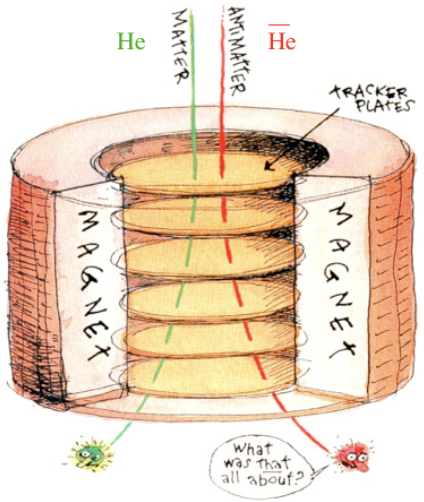

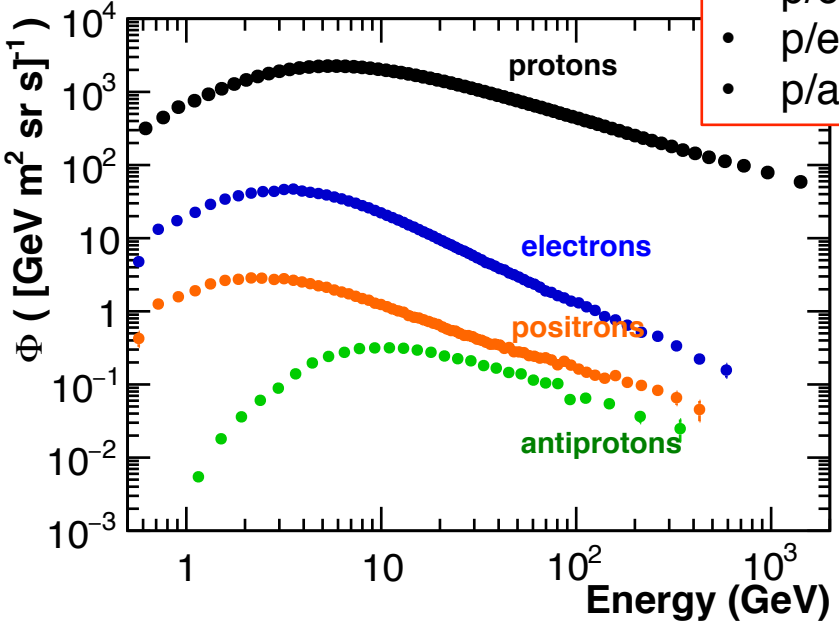

- $p/e^- \sim 10^2$
- $p/e^+ \sim 10^3$
- $p/antip \sim 10^4$

Particle identification is fundamental for antimatter measurements

Particle Identification

- Particles are uniquely identified by their **velocity**, **momentum** and **sign of the charge** combining the information from several subdetectors
- Curvature in magnetic field $\rho \propto R = \frac{p}{Ze}$
- Velocity after time of flight measurements $\beta \propto \frac{1}{\Delta T}$
- Ionization losses $\frac{\mathrm{d}E}{\mathrm{d}X} = f(z, \beta)$
- Calorimetric measurements $E_{kin} = (\gamma - 1)mc^2$
- Typically, measurements are more than the number of searched parameters → multiple measurements used to over-constrain the values and to crosscheck systematic effects
- NB: at high energies (β-->1), the sensitivity of velocity measurements decreases. Complementary techniques used to infer the particle energy.

Ionization energy losses

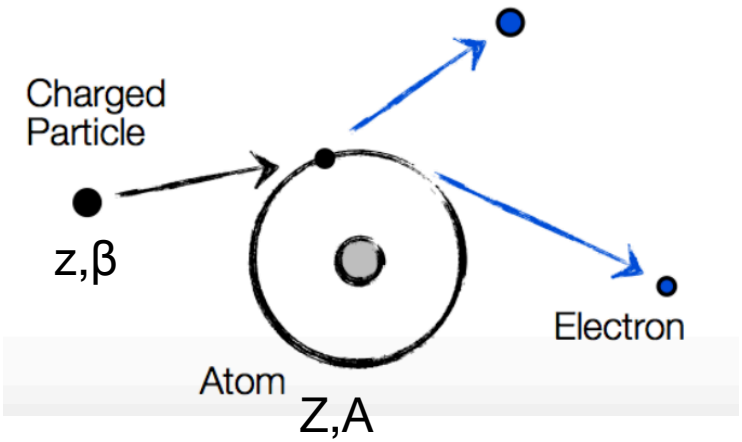

Main effect of energy loss in materials:
continuous energy losses by ionization from scattering off atomic electrons

Scattering off electrons: high energy losses, small trajectory deviation
Scattering off nuclei: small energy losses, high scattering angles (multiple scattering)

Bethe-Block formula: energy loss per unit of grammage $X = \rho\, x$

$$\frac{\mathrm{d}E}{\mathrm{d}X} = 0.31\,\mathrm{MeV}/(\mathrm{g}/\mathrm{cm}^2)\, z^2\, \frac{Z}{A}\, \frac{1}{\beta^2} \left[\frac{1}{2} \log(f(\beta)) - \beta^2 - \delta(\beta\gamma) \right]$$

Energy loss depends on particle and medium properties.

$\frac{\mathrm{d}E}{\mathrm{d}X} \propto z^2$ proportionality to particle charge used to identify heavy nuclei

Ionization energy losses

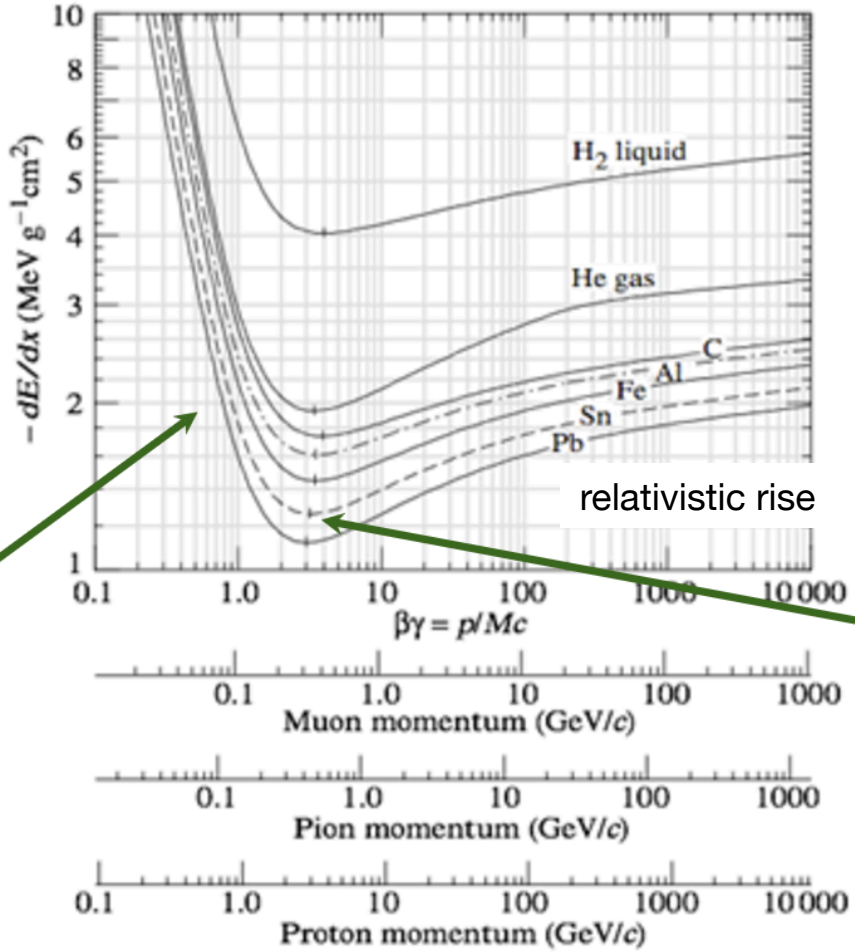

Figure 27.3: Mean energy loss rate in liquid (bubble chamber) hydrogen, gaseous helium, carbon, aluminum, iron, tin, and lead. Radiative effects, relevant for muons and pions, are not included. These become significant for muons in iron for $\beta\gamma \gtrsim 1000$, and at lower momenta for muons in higher-Z absorbers. See Fig. 27.21.

Bethe-Bloch formula:

$$-\frac{dE}{dx} = Kz^2\frac{Z}{A}\frac{1}{\beta^2}\left[\frac{1}{2}\ln f(\beta) - \beta^2 - \frac{\delta(\beta\gamma)}{2}\right]$$

Except in hydrogen, particles of the same velocity have similar energy loss in different materials.

The minimum in ionisation occurs at βγ = 3.5 to 3.0, as Z goes from 7 to 100

MIP: Minimum Ionizing Particle

PDG 2008

Minimum Ionizing particles

MIP dependence on chemical species

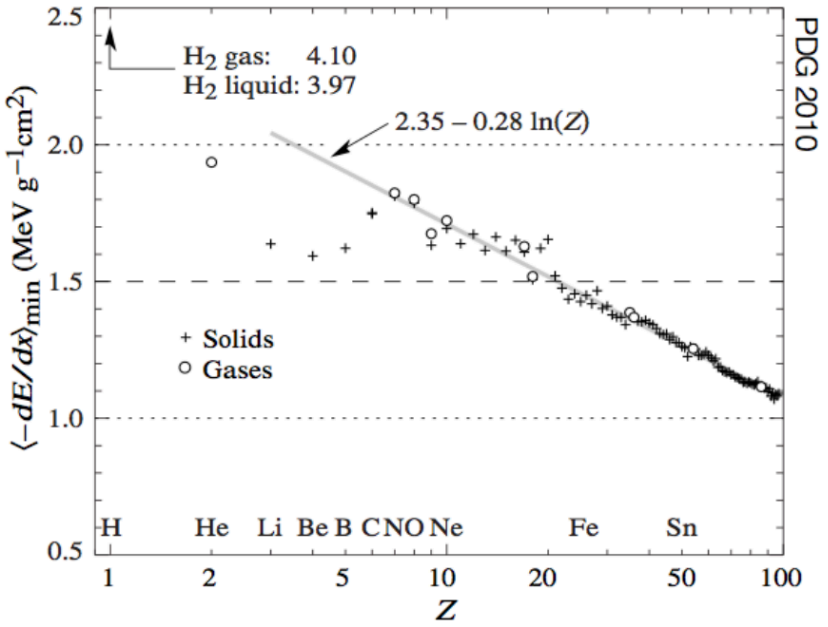

$$\frac{\mathrm{d}E}{\mathrm{d}X}_{|\mathrm{min}} \approx 1.5 \div 2\ \mathrm{MeV}/(\mathrm{g/cm}^2)$$

Below minimum: higher energy losses ~ $1/\beta^2$
Above minimum: energy loss approx. constant (relativistic rise)

At very high energies (above the "critical energy") radiative energy losses dominates.

- Real detector measures the energy ΔE deposited in a layer of finite thickness δx.
- For thick layers and high density materials:
  - Many collisions
  - Central limit theorem: distribution → Gaussian

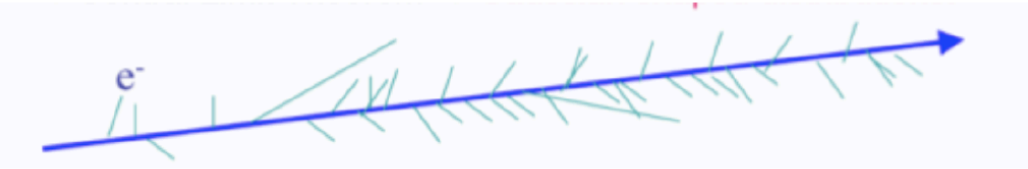

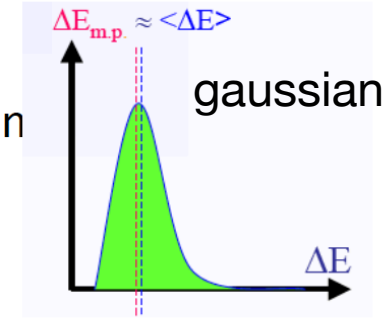

- For thin layers or low density materials:
  - Few collisions, some with high energy transfer.
  - ⇒ Energy loss distributions show large fluctuation towards high losses
  - ⇒ Long Landau tails

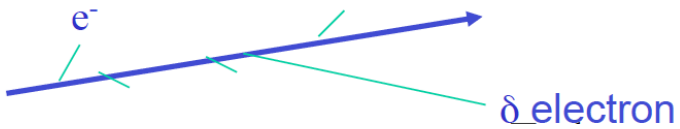

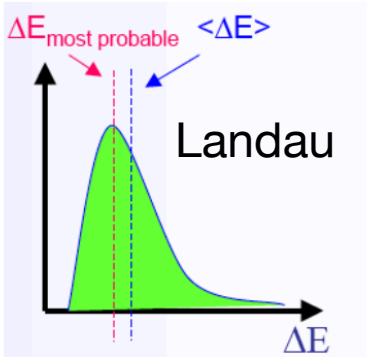

The most probable energy loss does not coincide with the average energy loss due to rare large angle scatterings.

The Bethe-Block formula describes the parametrization of the average energy losses

Multiple scattering

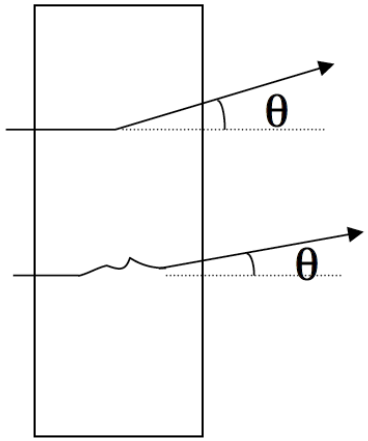

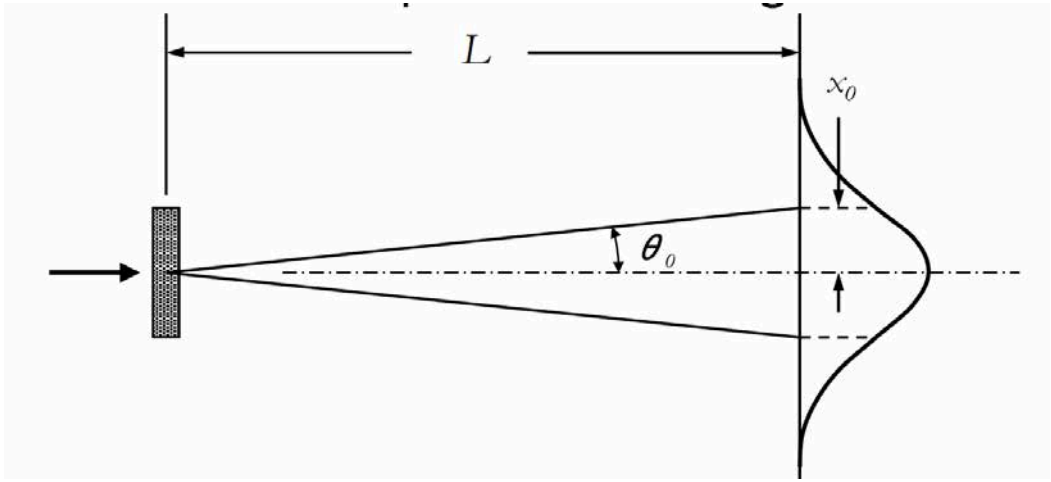

Many small angle deviations can result in a net angle when traversing a material slab

In average <θ>=0, but the distribution has a width

$$\theta_0 = \theta_{plane}^{RMS} \approx \frac{13.6MeV}{p\beta c} z\sqrt{\frac{L}{X_0}}$$

i.e. $$\theta_0 \propto \frac{1}{p}\sqrt{\frac{L}{X_0}}$$

Charge of incident particle

Radiation length of absorbing material

This results in a limit of resolution for tracking applications.
The less material, the better the tracking resolution.

Charge ID

$\frac{\mathrm{d}E}{\mathrm{d}X} \propto z^2$ charge proportionality used to identify heavy nuclei

Distribution of energy deposits can have long tails

Consequence: multiple measurements of energy deposits are needed to sample the Landau distribution and correctly infer the particle charge

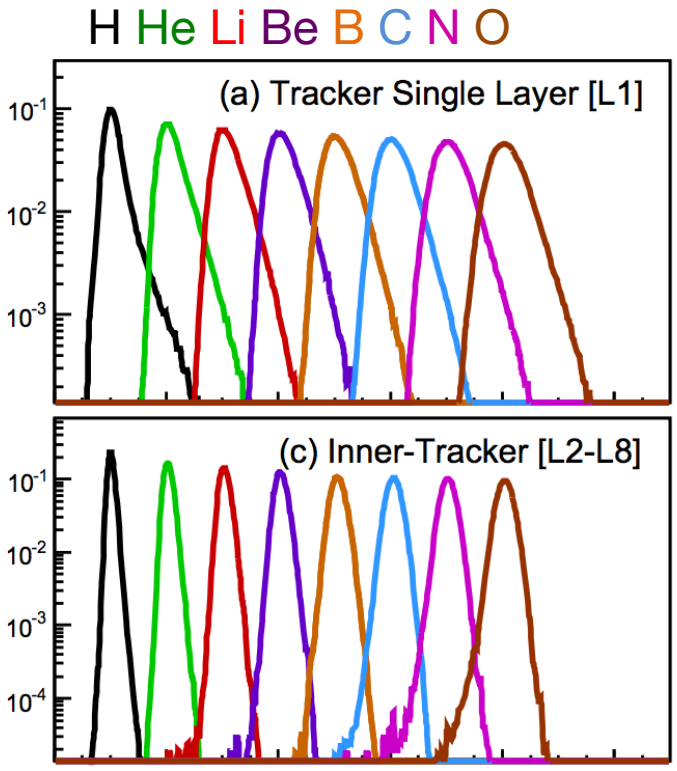

Charge sampled in one layer of silicon
"Landau" distribution, long tails

Charge sampled in seven layer of silicon
Estimator built using mean / truncated mean / likelihood
--> Charge resolution improved

dE/dX measurements

Scintillators

Conversion of ionization energy in photons detected with photodetectors

Organic/plastic scintillators:
- low Z, density = 1 g/cm3
- fast (ns)
- low light yield
- used for timing applications

Inorganic/crystal scintillators:
- high Z, dense
- slow
- high light yield
- used for calorimetric applications

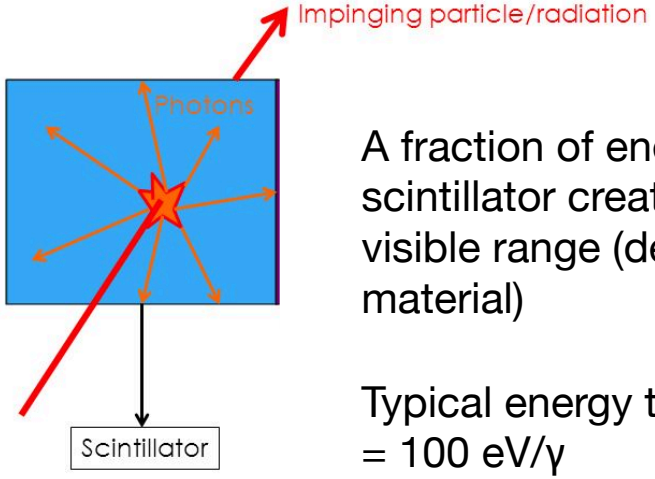

A fraction of energy deposited in the scintillator creates photons in the visible range (details depend on the material)

Typical energy to create one photon = 100 eV/γ

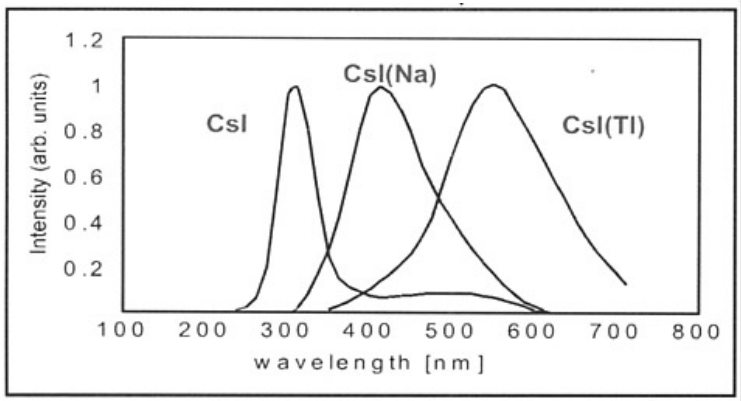

dE/dX measurements

Scintillators

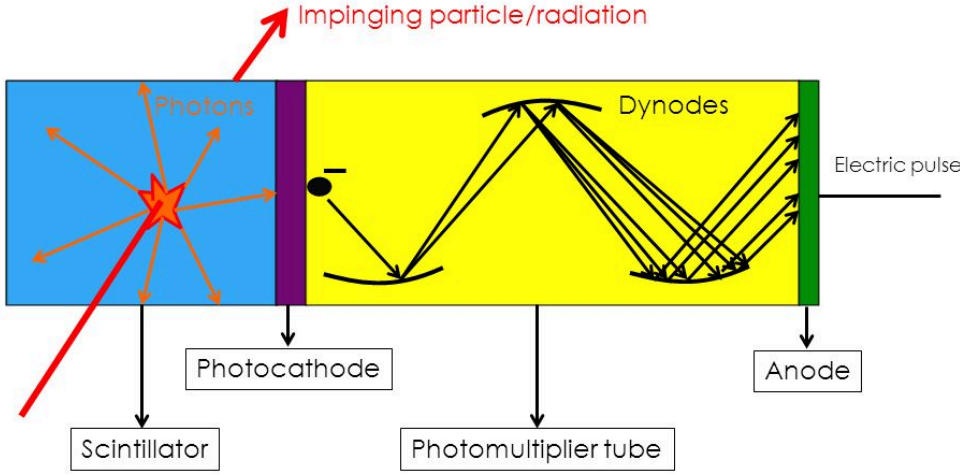

Photomultipliers (PMT) convert photons in measureable electric pulses

$$I_{PMT} \propto N_\gamma \propto \Delta E$$

Photocathode: photons generate a free photoelectron via photoelectric effect

Dynodes: d.d.p. (kV) between dynodes accelerates electrons. Electrons hitting dynodes may generate a number (approx 3-5) of free electrons to be accelerated

Anode: at the end of many diodes (approx. 10), electrons are collected

For each photoelectron, approx. 10^7 electrons are collected at the anode (gain of the PMT)

Photo-detection efficiency < 30% for PMTs

dE/dX measurements

Scintillators

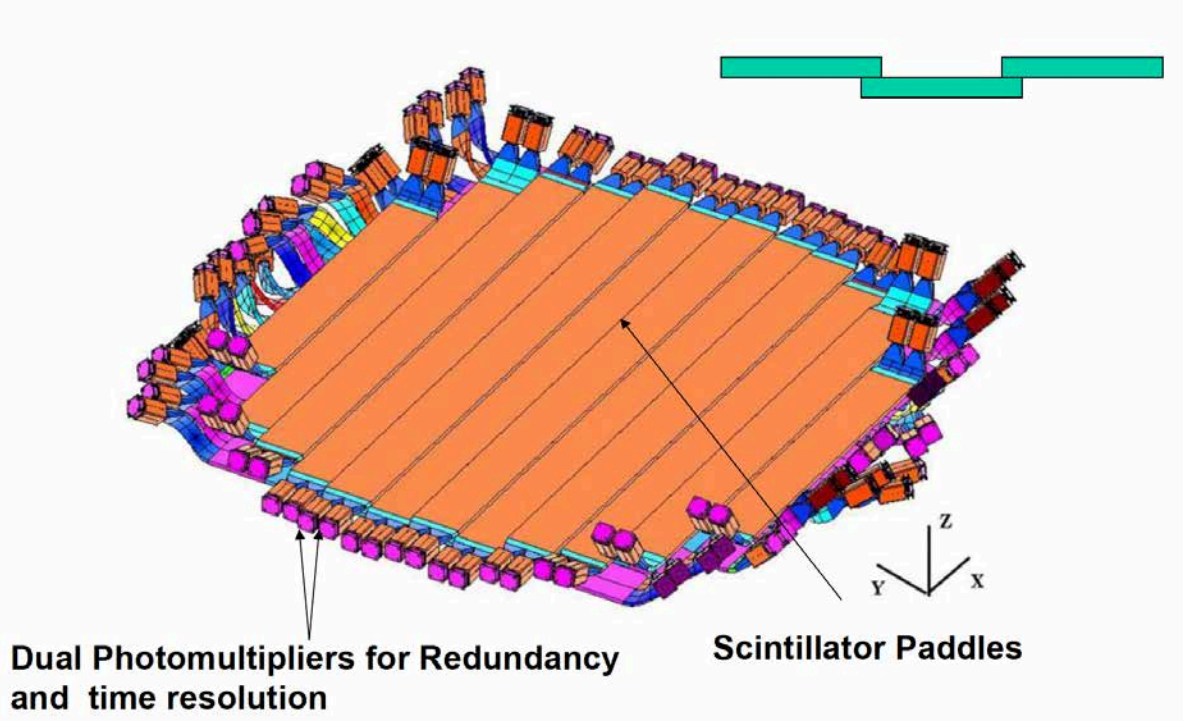

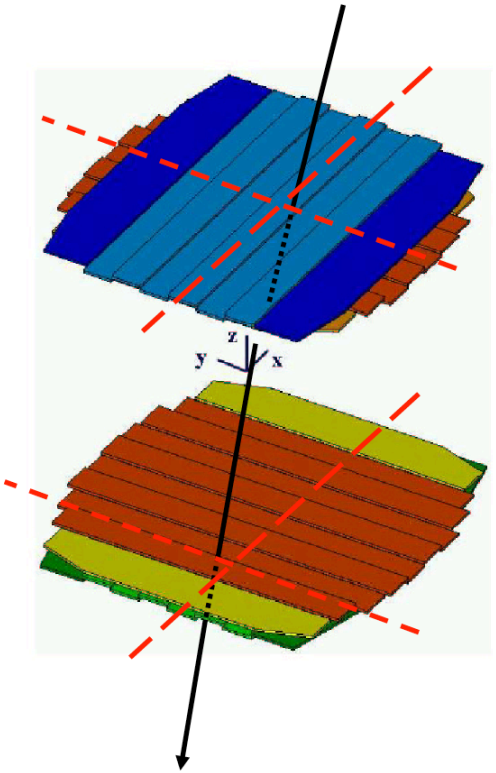

Plastic scintillators are used in space detectors as planes to "**trigger**" (i.e. start) the data acquisition of the whole detector

Time coincidence between different planes used as fast trigger signal

Time of flight

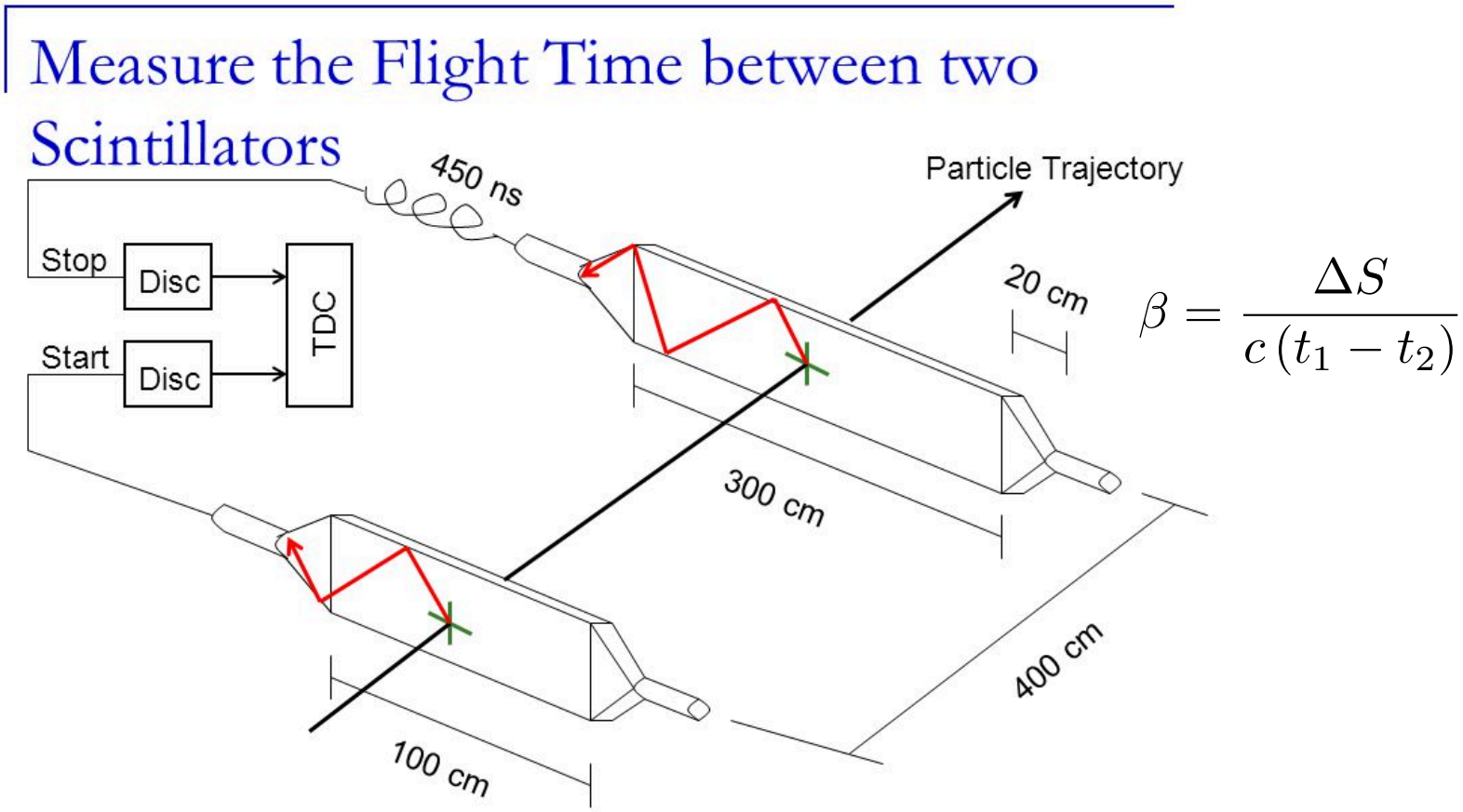

- Path of relativistic particles: 30 cm/ns
- Typical spans are order of 1m → time resolution of ns are needed to measure the particle velocity up to c
- Fast Scintillators coupled to fast photodetectors (PMT, SiPM) are commonly used

dE/dX measurements

Solid state detectors

p-n junction

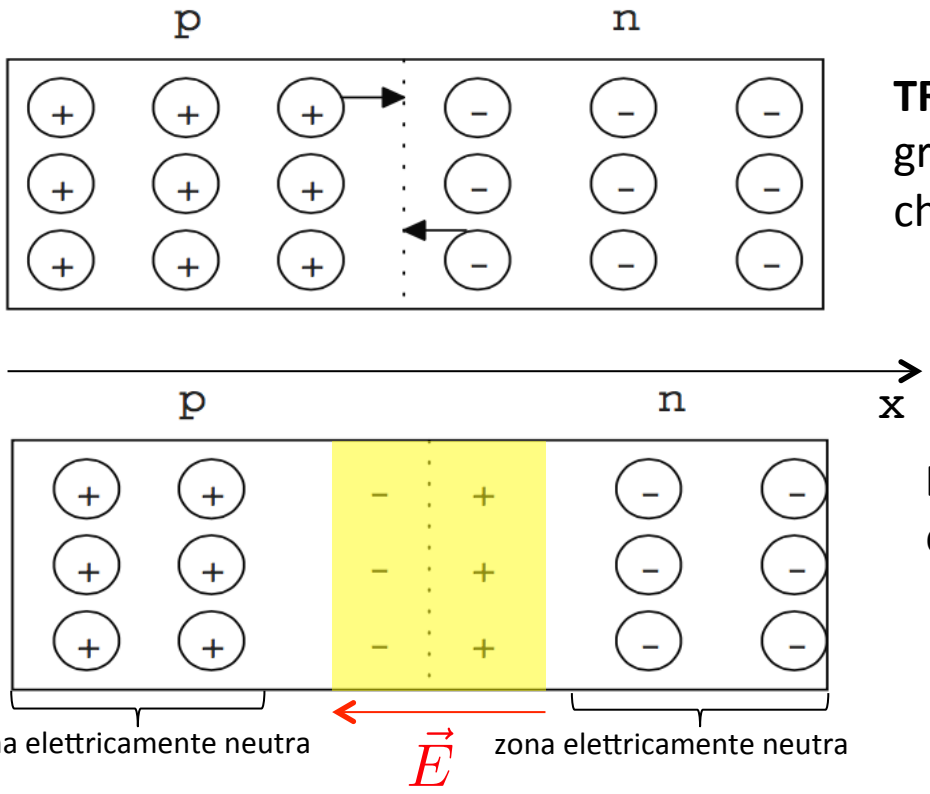

TRANSIENT:
gradient of concentration --> **diffusion** of charge carriers

EQUILIBRIUM:
creation of space charge zone

depleted zone: no charge carrier, net electric charge!=0
P and N zone: charge equilibrium, net electric charge=0

dE/dX measurements

Solid state detectors

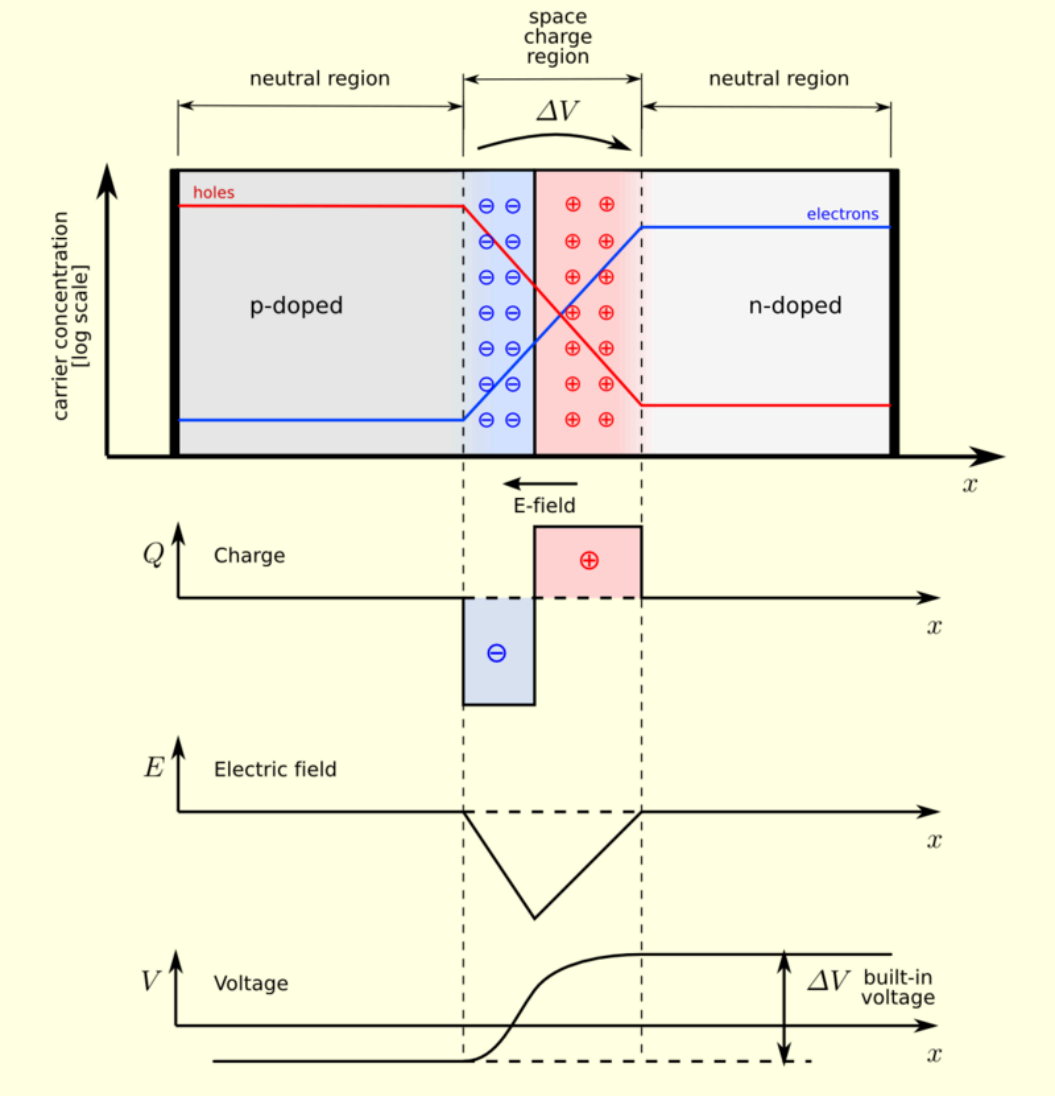

dE/dX measurements

Solid state detectors

The depletion zone is maximized by application of a reverse bias voltage

Through going charged particles create $e^- h^+$ pairs in the depletion zone (about 30.000 pairs in standard detector thickness). These charges drift to the electrodes. The drift (current) creates the signal which is amplified by an amplifier connected to each strip. From the signals on the individual strips the position of the through going particle is deduced.

The charge is collected in one (or few more strips) -> this provides information on the particle crossing position

Strip readout pitch approx 100μm (or less) -> can achieve **position resolution down to 10μm or better** using center of gravity of energy deposit.

The amount of charge, proportional to the ionization and to Z^2, is used to infer the charge of the particle

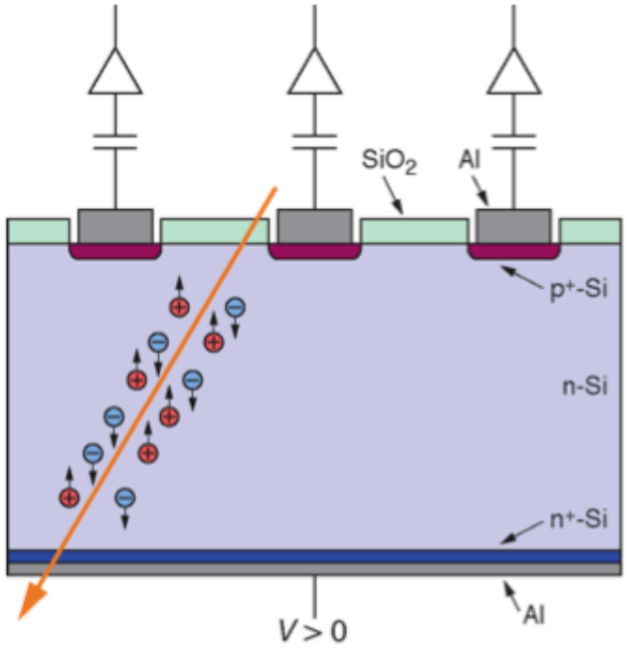

dE/dX measurements

Solid state det

A charged particle crosses a thin layer of n-doped silicon (typically 300µm) and interacting with the material frees in average 100 e/h pairs per µm, for a total of $30 \cdot 10^3$ pairs in 300µm

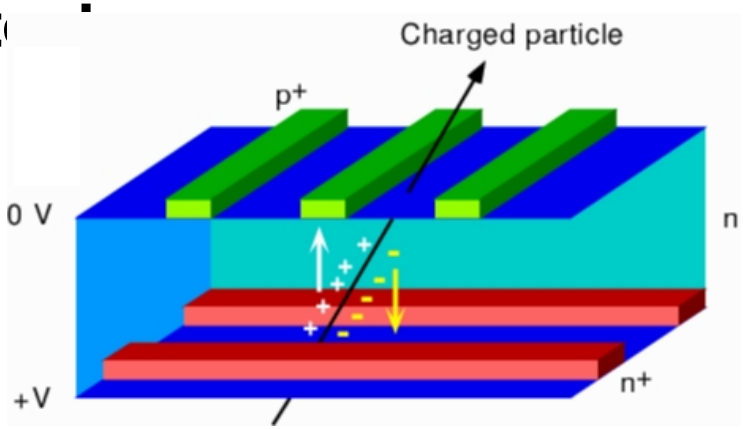

In the silicon surface, thin p+ strips are implanted (c.a. 10µm every c.a. 100µm). The p+/n system is kept in reverse polarization. Less than 100V are needed to completely deplete the silicon bulk.

The e/h pairs are collected on the opposite sides of the silicon.
In some cases, n+ strips are added running in the opposite direction on the opposite side of p+ strips (**double sided silicon**). This allows the measurement of both coordinates.

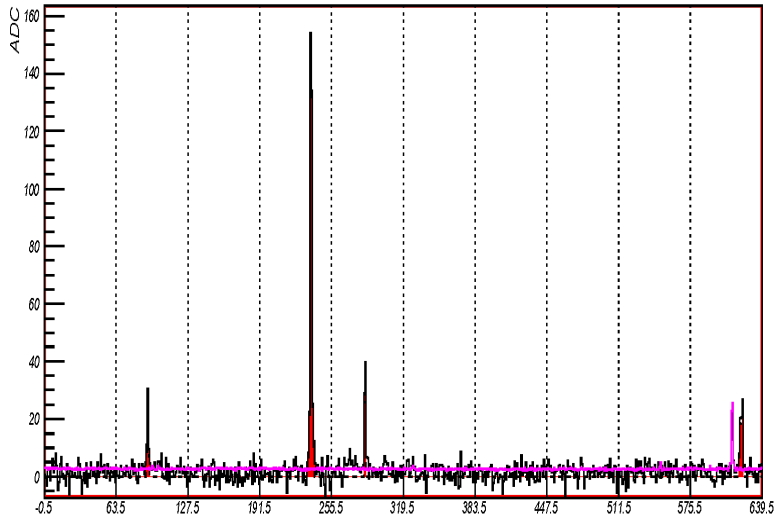

Coordinata
(in "canali", da convertire in posizione)

Spectrometers

Magnetic Spectrometers

Simple 2D sagitta model

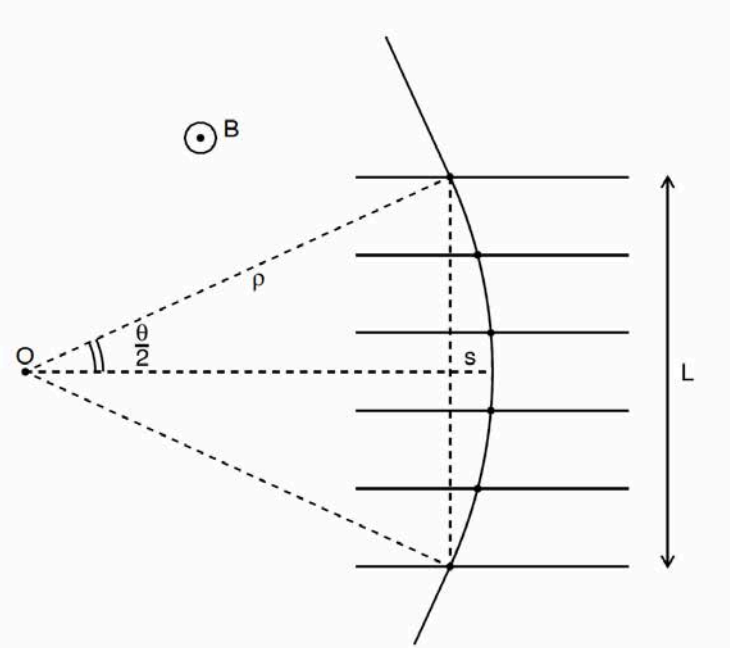

- Charged particle bent in magnetic field
- The sagitta is measured by sampling the particle trajectory through different planes

- Master formula of charged particle in MF

$$R(\mathrm{GeV}) = q\,B\,\rho = 0.3\,B(\mathrm{T})\,\rho(\mathrm{m})$$

- Rigidity $R = p/Ze$ defines the particle trajectory in a magnetic field

Spectrometers

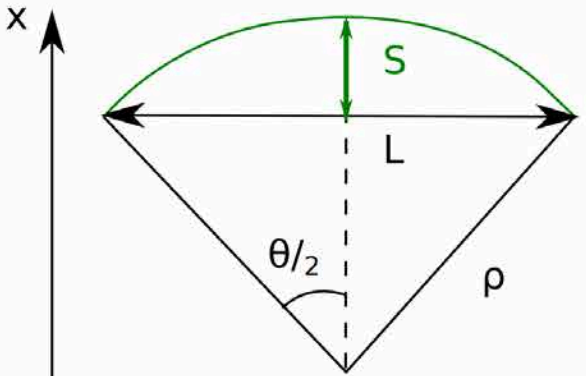

$$\theta \approx L/\rho = qBL/p$$

$$\text{Sagitta} \quad S = \rho - \rho\cos\frac{\theta}{2} = \rho\left(1-\cos\frac{\theta}{2}\right) = 2\rho\sin^2\frac{\theta}{4}$$

$$\text{for small } \theta \quad S \simeq \frac{\rho\theta^2}{8}$$

$$s(m) = \frac{0.3\,B\,L^2}{8\,p}$$

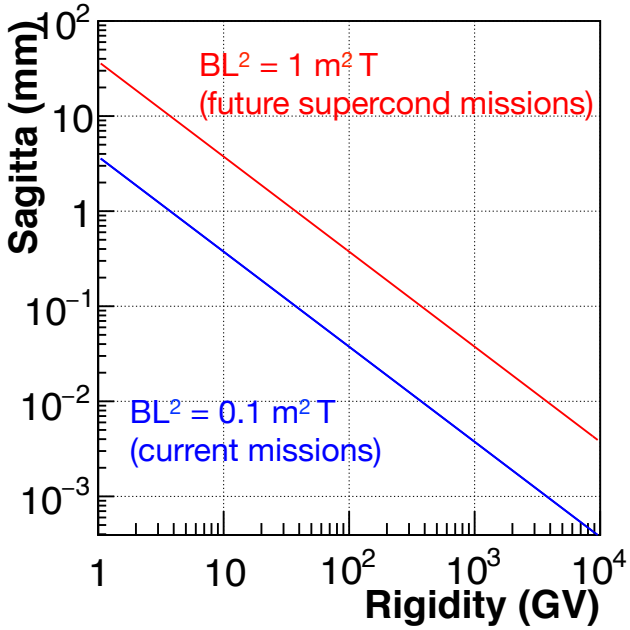

BL² "Bending power": characteristic parameter of spectrometer performance

Spectrometers

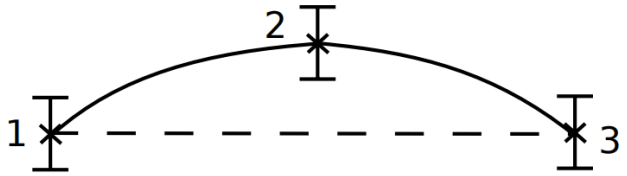

Sagitta defined by the measurement of at least 3 points. The error on the sagitta is determined by the accuracy of the coordinate measurement

$$s = \frac{x_1 + x_3}{2} - x_2 \quad \sigma^2(s) = \frac{\sigma^2(x)}{4} + \frac{\sigma^2(x)}{4} + \sigma^2(x) \quad \sigma(s) = \sqrt{\frac{3}{2}}\sigma(x)$$

$$\frac{\sigma(p)}{p} = \frac{\sigma(R)}{R} = \frac{\sigma(s)}{s} = \sqrt{\frac{3}{2}}\frac{8\,\sigma(x)}{0.3\,B\,L^2} \cdot p$$

$$\frac{\sigma(p)}{p} \propto p,\ \sigma(x),\ \frac{1}{B\,L^2}$$

Spectrometer resolution worsens at high rigidities and can be improved by better coordinate measurement accuracy and better bending power

- L ~ Spectrometer dimensions, limited by the space constraints
- B, limited by magnet size and technology (superconducting magnet in space?)
- σ(x) ~ position resolution → experimental effort to achieve resolutions below 10μm

Spectrometers

Magnetic Spectrometers

Simple 2D sagitta model

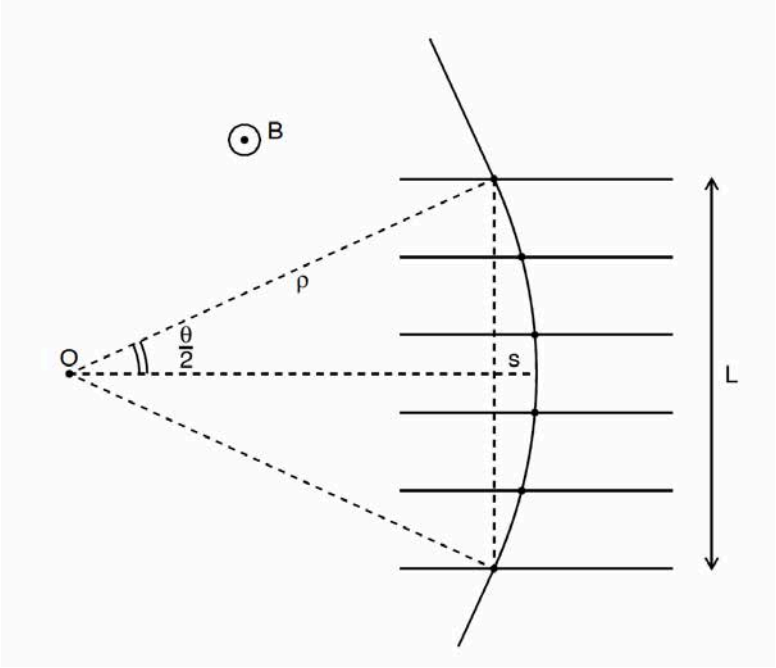

- Charged particle bent in magnetic field
- The sagitta is measured by sampling the particle trajectory through different planes
- The particle rigidity is inferred via

$$R(GV/c) = \frac{0.3\,B(T)\,L(m)^2}{8\,s(m)}$$

- Rigidity resolution scale linearly as

$$\frac{\sigma_R}{R} = \frac{\sigma_s}{s} \propto R$$

- Maximum Detectable Rigidity MDR

$$\frac{\sigma_R}{R} = 1 \;\Rightarrow\; R^{(\mathrm{MDR})} \propto \frac{L^2 B}{\sigma_s}$$

- L ~ **Spectrometer dimensions**, limited by the space constraints
- B, limited by **magnet size and technology** (superconducting magnet in space?)
- σ_S ~ **position resolution** → experimental effort to achieve resolutions below 10μm

Spectrometers

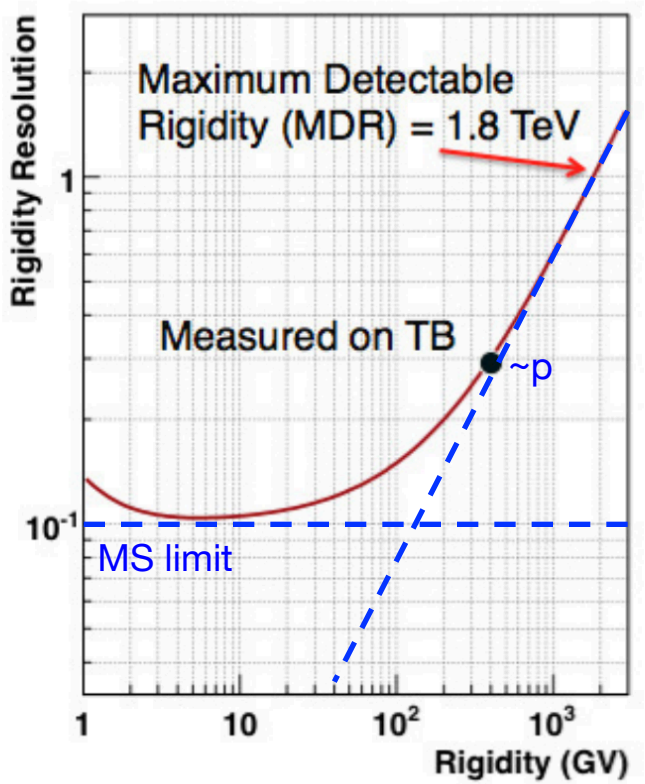

Performance parameter:
Maximum Detectable Rigidity (MDR):

$$\frac{\sigma_R}{R} = 1 \Rightarrow R^{(\mathrm{MDR})} \propto \frac{L^2 B}{\sigma_s}$$

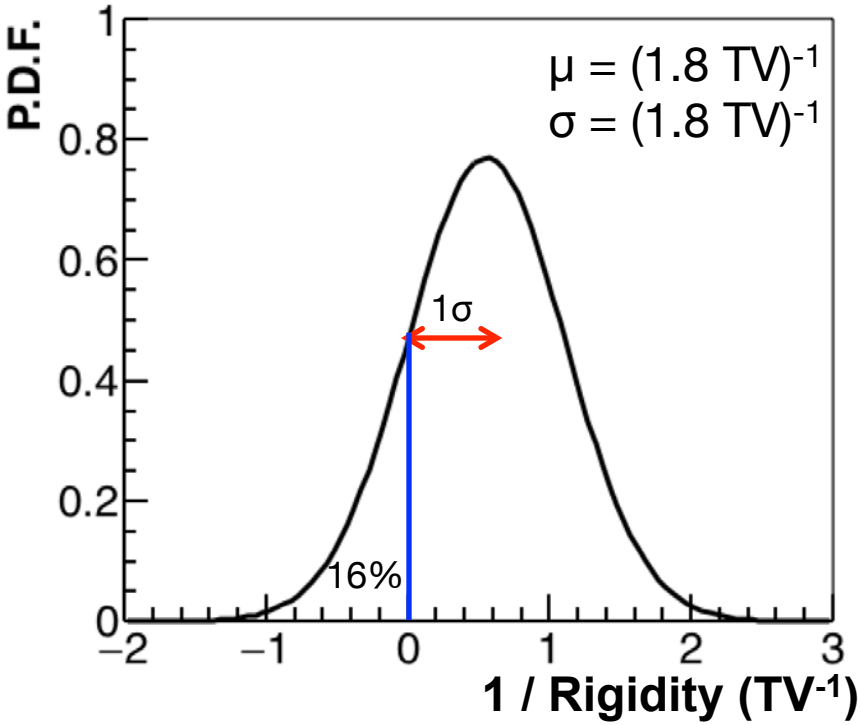

At high energies $\frac{\sigma(p)}{p} \propto p$

At low energies (Multiple scattering) $\frac{\sigma(p)}{p} \approx \mathrm{cost}$

"Spillover": events that are reconstructed with opposite sign of charge

Silicon Microstrip Detectors

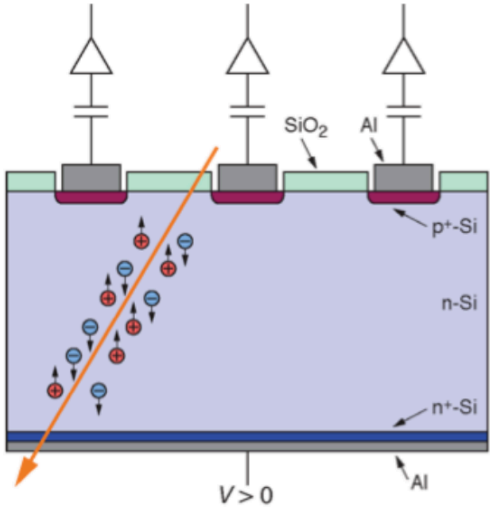

Amplitude → Z^2

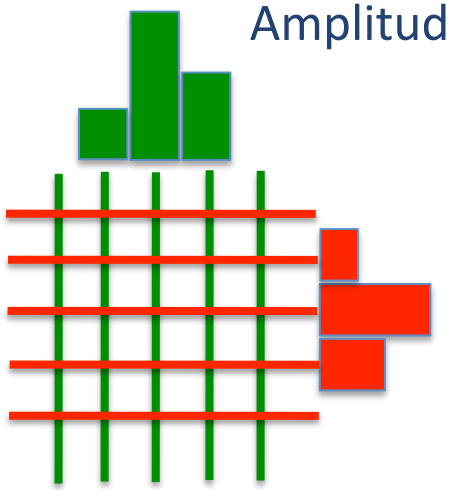

Position from the center of gravity of the signal released on adiacent strips (50-200 μm)

Single sensor ≈ 10x10cm^2 … or less

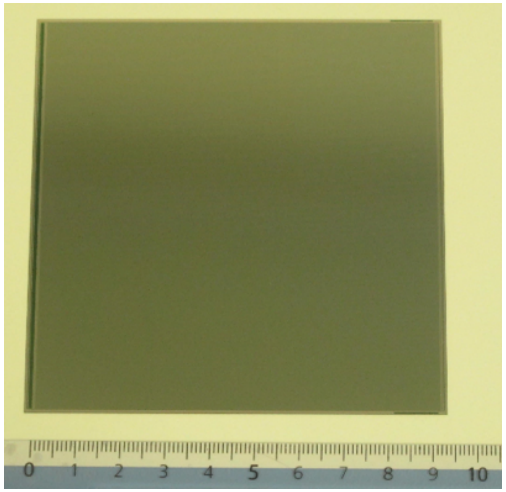

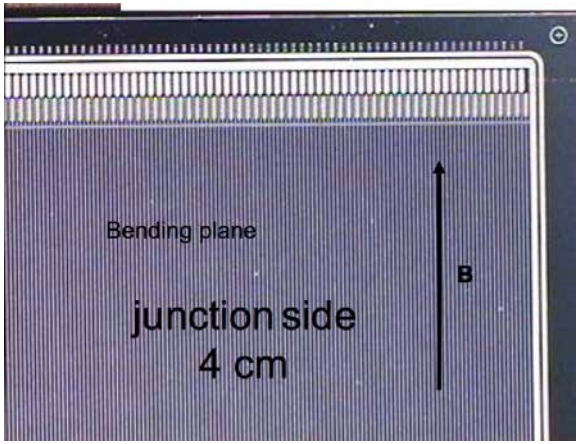

AMS-01: First magnetic spectrometer with a silicon tracker in space

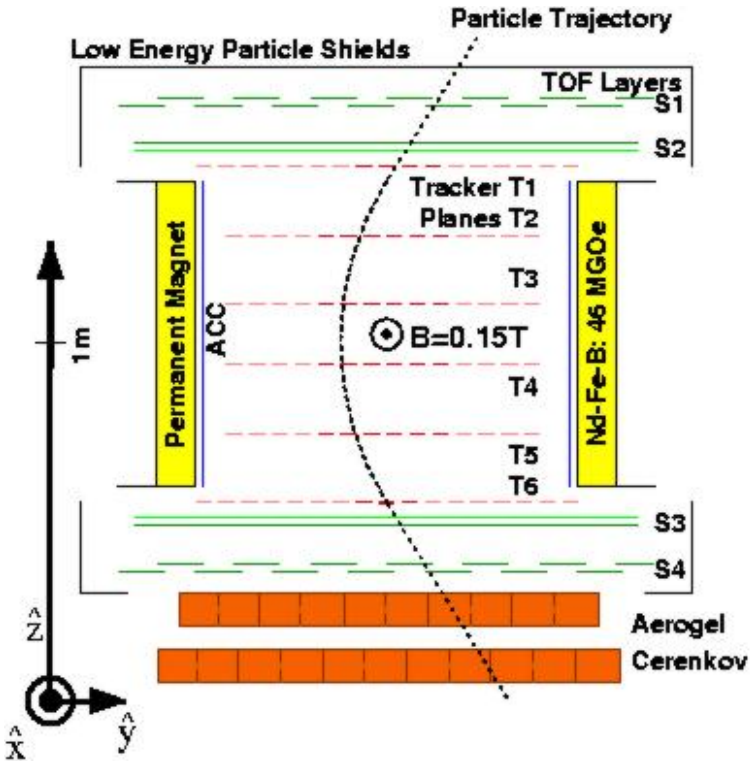

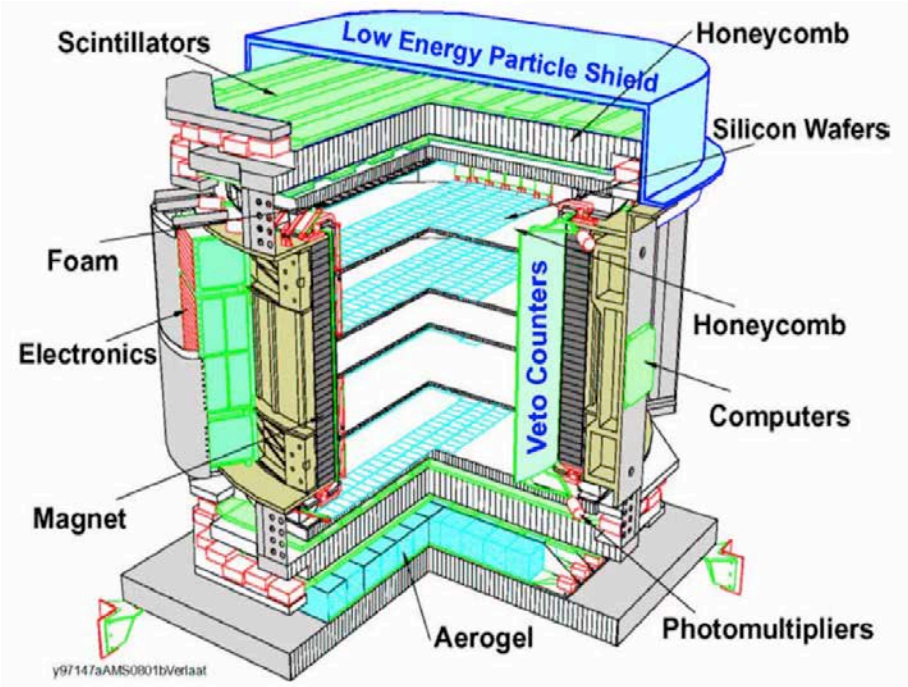

Time Of Flight : measure time → velocity, arrival direction, dE/dX → Z

Magnet: 2.2 Ton of Nd-Fe-B blocks providing a 15kGauss field inside, < 2 Gauss outside

Tracker: 2m² of silicon sensors arranged in 6 planes

Aerogel Cerenkov threshold counter: discrimination of e/p based on Cherenkov emission

Fermi (2008)

73m^2 of silicon sensors in space

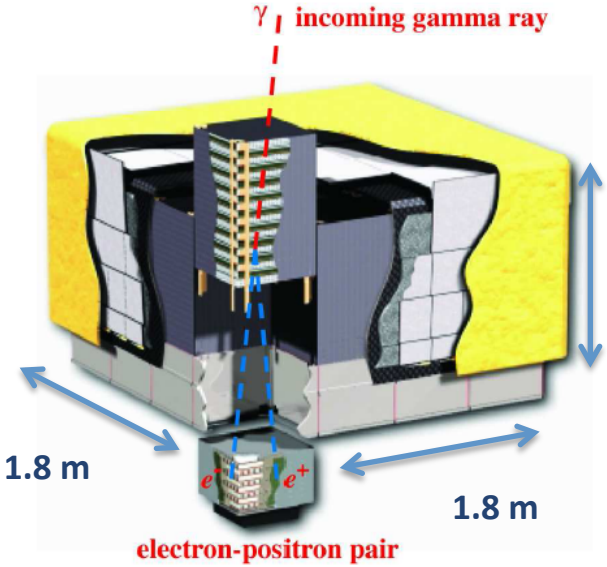

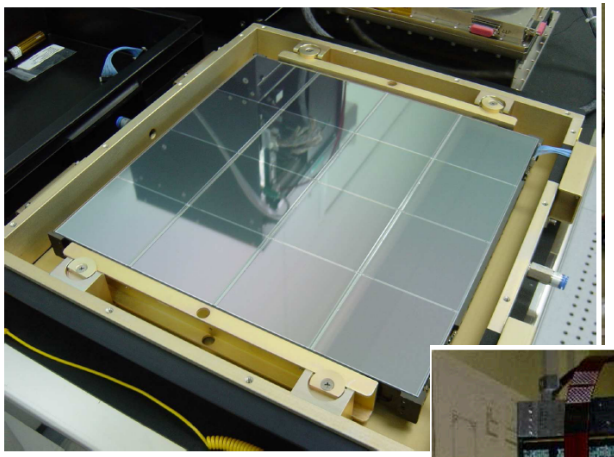

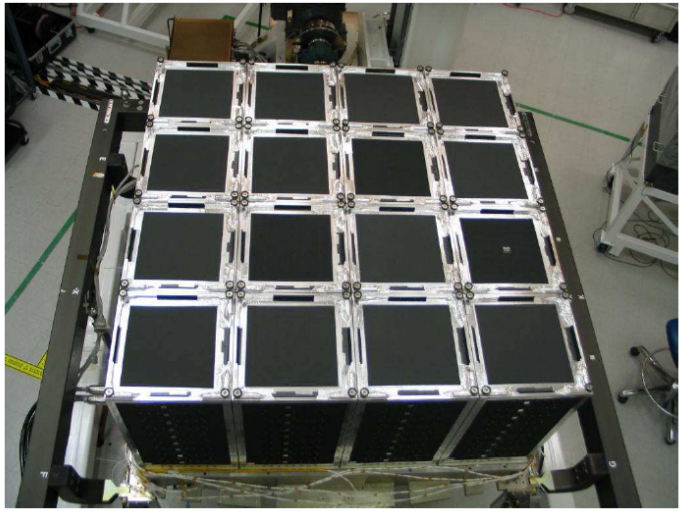

AMS-02 (2011)

9 planes of silicon sensors in space (6.4 m^2)

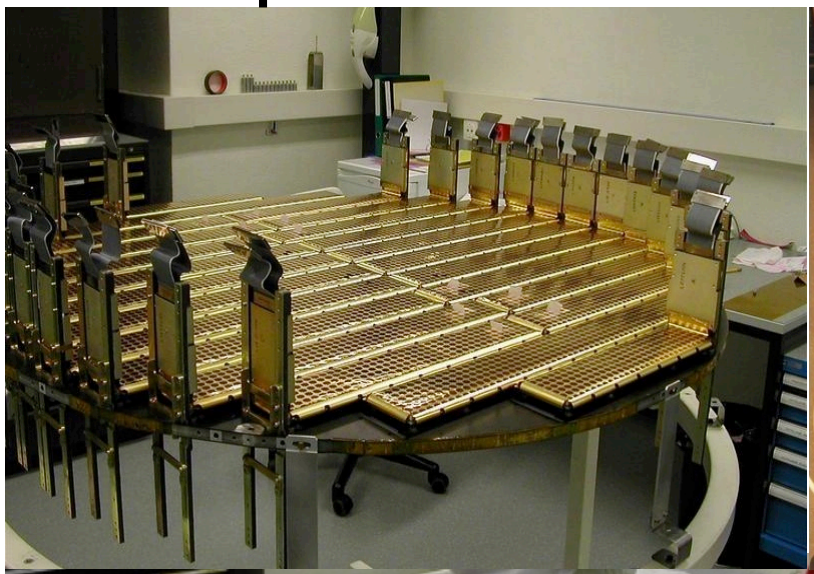
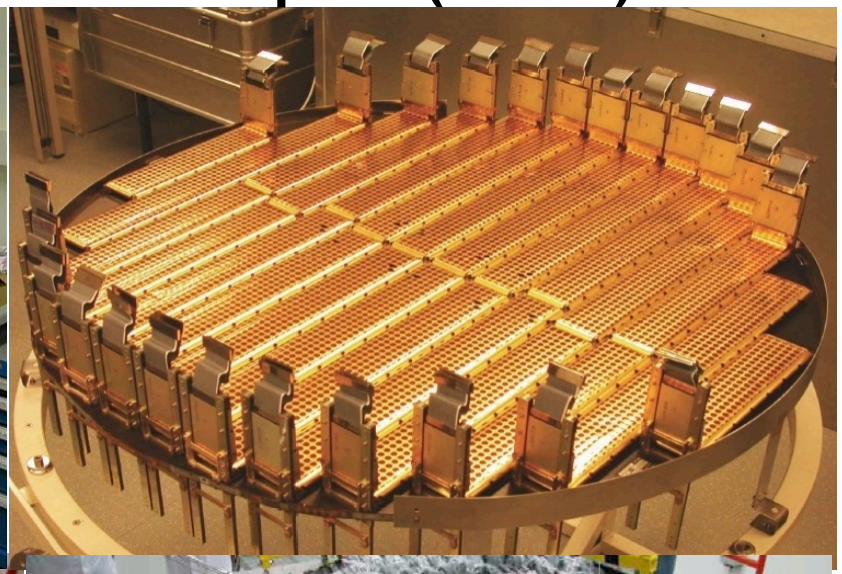
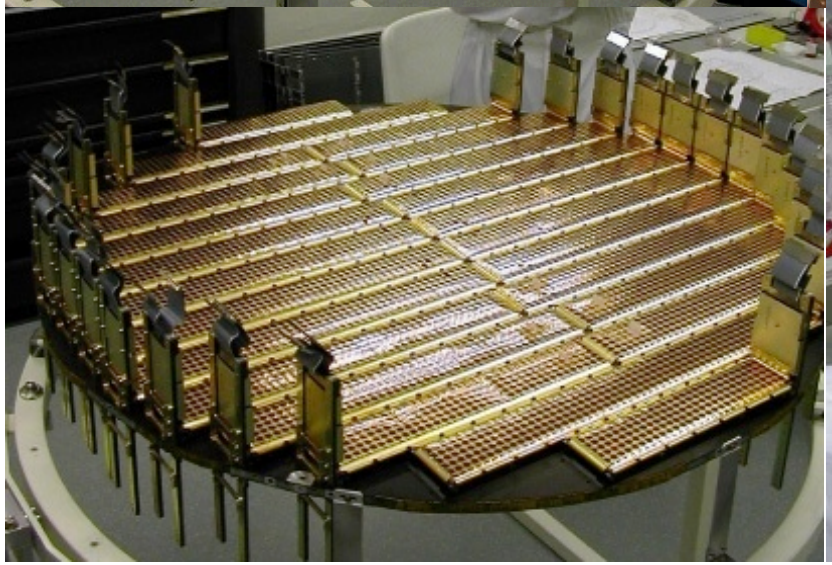


DAMPE (2015)

6 planes of silicon sensors in space (7.7 m^2)

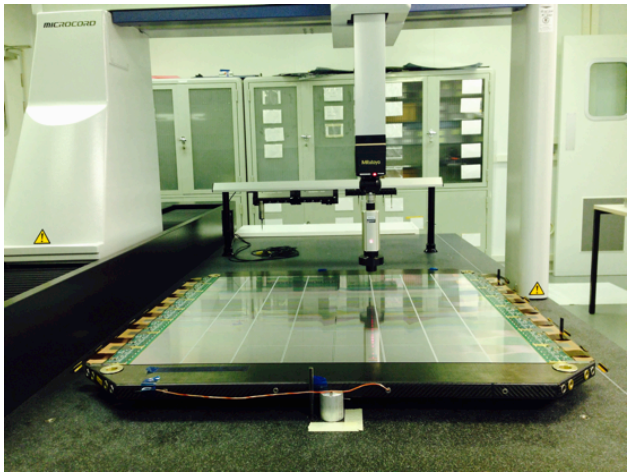

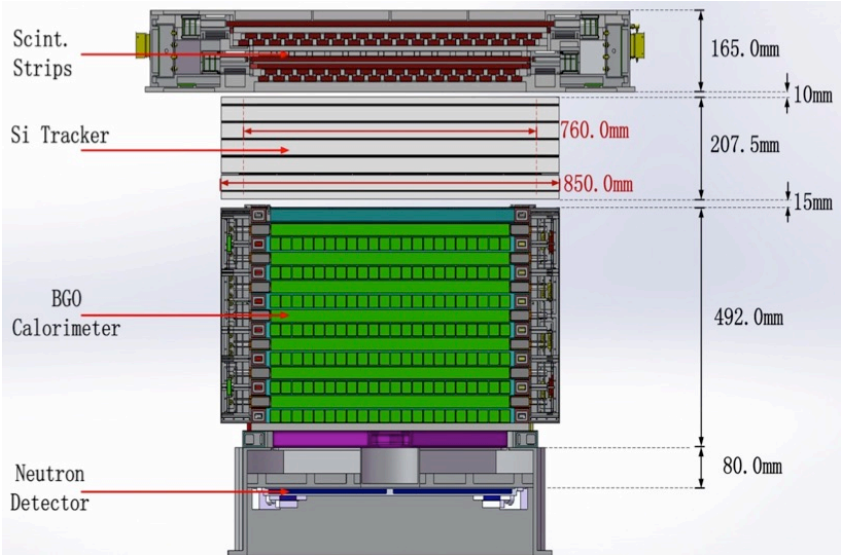

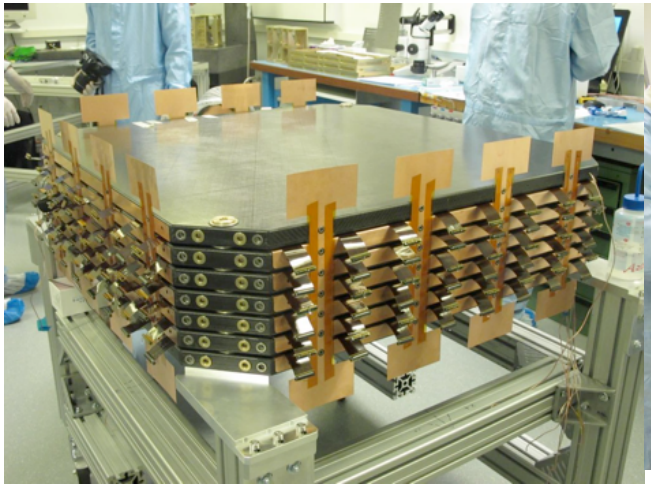

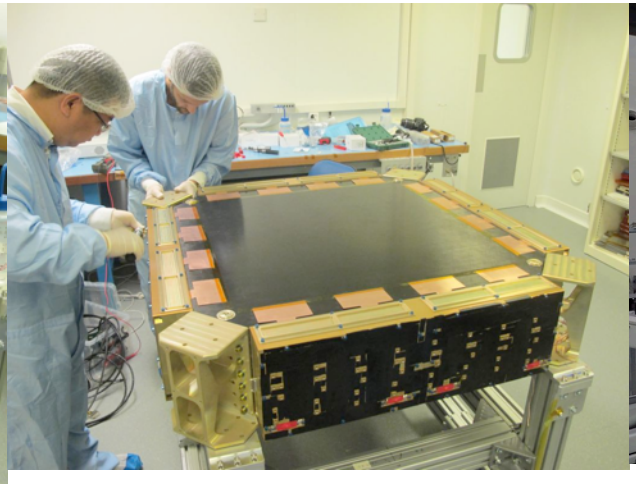

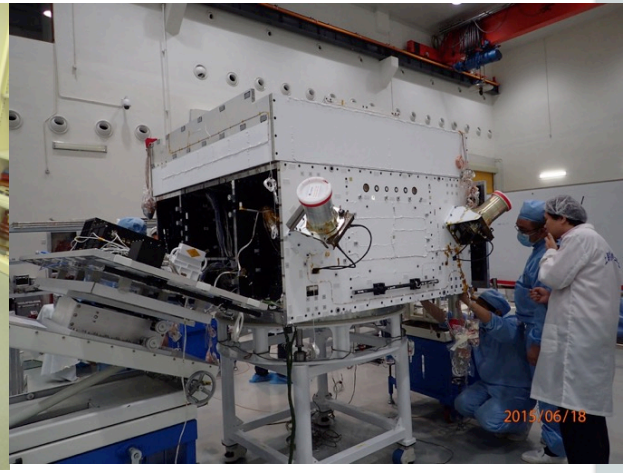

Calorimetry

- **Calorimeters: instruments in which particles are partially or completely absorbed to measure their energy**

- Electromagnetic calorimeters (homogeneous, sampling)
- Hadronic calorimeters (sampling)

- Destructive detectors, sited at the “end” of the detector.

- Many techniques and technology, depending on the particle to be measured. We focus only on the simpler electromagnetic calorimeters for high energy particles

Electron radiative energy losses

- Electrons differ from other charged particles due to their lighter mass.

- A charged particle accelerated in an electromagnetic field release energy.
- Classical description: $\frac{\mathrm{d}E}{\mathrm{d}t} = \left(\frac{2}{3}\frac{e^2}{c^3}\right) a^2$

Relativistic electrons accelerated in the electric field of a nucleus radiate energy via the **Bremssstrahlung** effect.

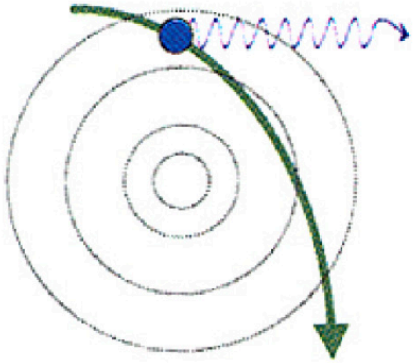

In a continuous medium, the losses are continuous and the electron energy degrades as $E(x) = E_0\, e^{(-x/X_0)}$

X_0 (radiation length) = typical length scale of radiative energy losses

$$X_0 = \frac{716.4 \cdot A}{Z_2^2 \ln \frac{287}{Z_2^{1/2}}} \qquad \left(g/cm^2\right)$$

Energy losses

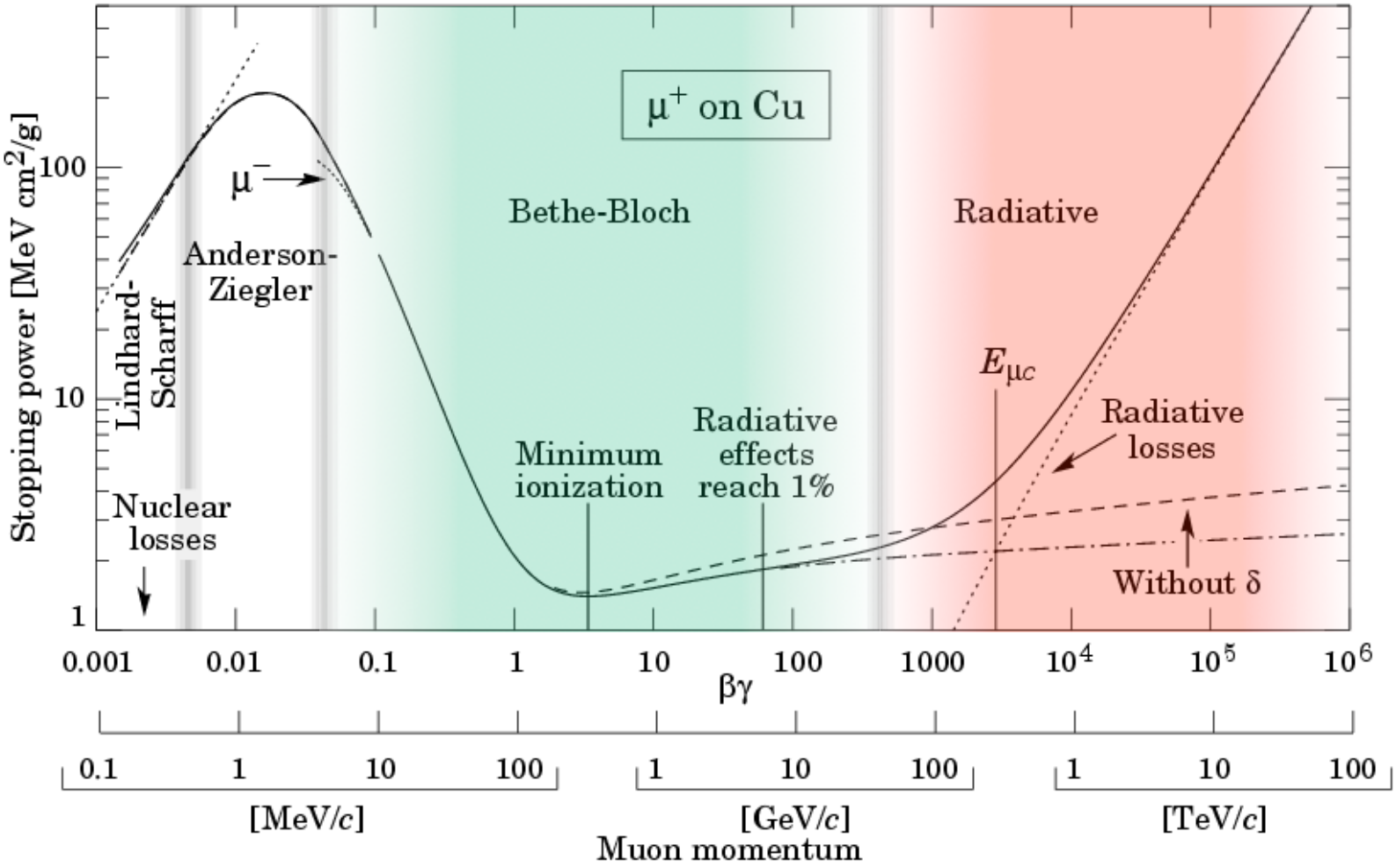

Critical energy: $\left(\frac{\mathrm{d}E}{\mathrm{d}x}\right)_{ion} = \left(\frac{\mathrm{d}E}{\mathrm{d}x}\right)_{brem}$

$$E_C \approx 700/(Z+1)\ \mathrm{MeV}$$

$$E_C \propto \frac{1}{m^2} \Rightarrow E_C(\mu) \approx 4 \cdot 10^4\, E_C(e)$$

Interactions of photons

- For low energies (500 keV ≥ E_γ ≥ ionisation energy) the photoelectric effect dominates,

  $\gamma + \text{atom} \rightarrow \text{atom}^+ + e^-$

- In the range of medium energies ($E_\gamma \approx 1$ MeV) the Compton effect, which is the scattering of photons off quasi-free atomic electrons,

  $\gamma + e^- \rightarrow \gamma + e^-$

  has the largest cross section,

- and at higher energies ($E_\gamma \gg 1$ MeV, typically 50 MeV) the cross section for pair production dominates,

  $\gamma + \text{nucleus} \rightarrow e^+ + e^- + \text{nucleus}$

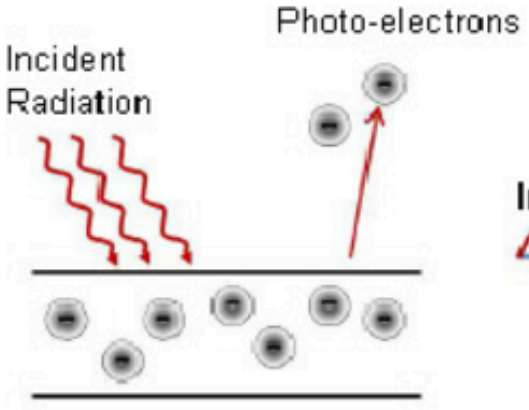

$$E_e = E_\gamma - W_e$$

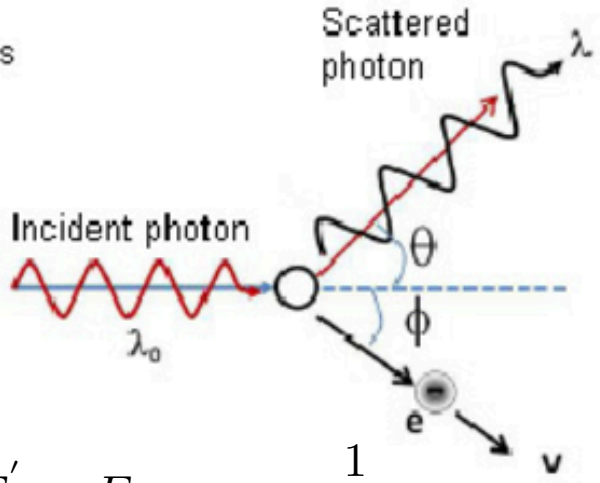

$$E'_\gamma = E_\gamma \frac{1}{1 + \frac{E_\gamma}{m_e}(1 - \cos(\theta))}$$

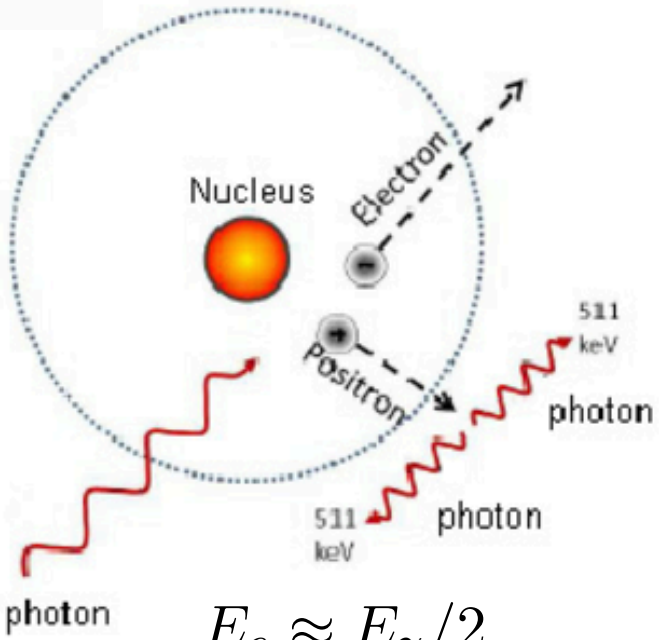

$$E_e \approx E_\gamma / 2$$

Interactions of photons

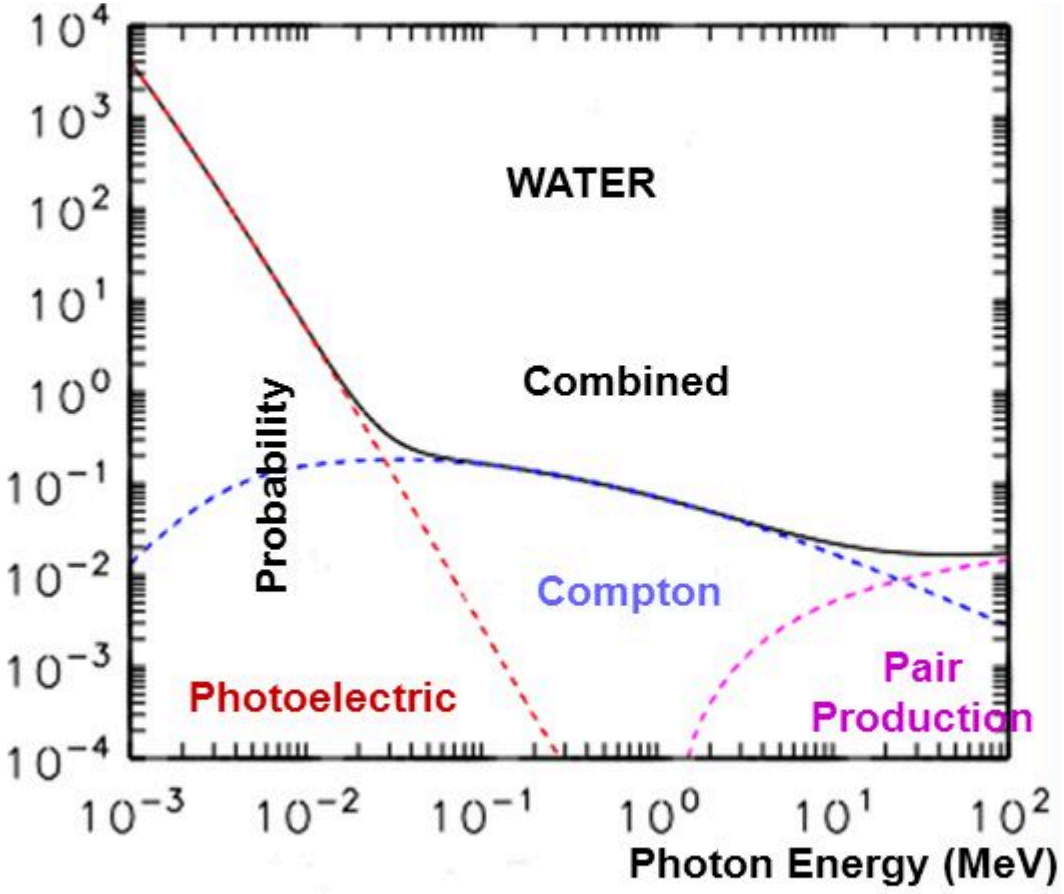

The profile strongly depends on the material, but in general above the pair production energy threshold ($E_{th} = 2m_e$) pair production rapidly becomes the dominating energy loss mechanisms for photons

Calorimetry

- A causa del bremsstrahlung, un fascio di $e^{\pm}$ di energia iniziale E_0, dopo un tratto x di materiale ha un'energia:

$$E = E_0 e^{-x/X_0}$$

- In un mezzo omogeneo di lunghezza di radiazione X_0, a causa della produzione di coppie, l'intensità di un fascio monocromatico di γ, diminuisce dopo un tratto x di materiale:

$$I = I_0 e^{-(7/9)x/X_0}$$

NB: nel primo caso il numero di e- e' costante, cambia l'energia delle particelle, non il loro numero. Nel secondo, l'energia dei fotoni rimane la stessa ma scompaiono particelle

Electromagnetic showers

The physics of e-m. shower is well known (hadronic showers are more complicated)
Simplest parametrization by Rossi describes the main shower properties.
More accurate descriptions involve Monte Carlo simulations.

Lo sciame è creato da e^+, e^- che emettono γ per BREMS e γ che creano coppie e^+, e^-

- Questi processi avvengono a distanza di 1 X_0
- In ogni processo $E = E_i / 2$

Alla distanza X abbiamo n processi avvenuti con:

- $n = X/X_o$
- $E_s = E_0/2^n$
- $N_s = 2^n$

La valanga si ferma ad $E_s = E_c$

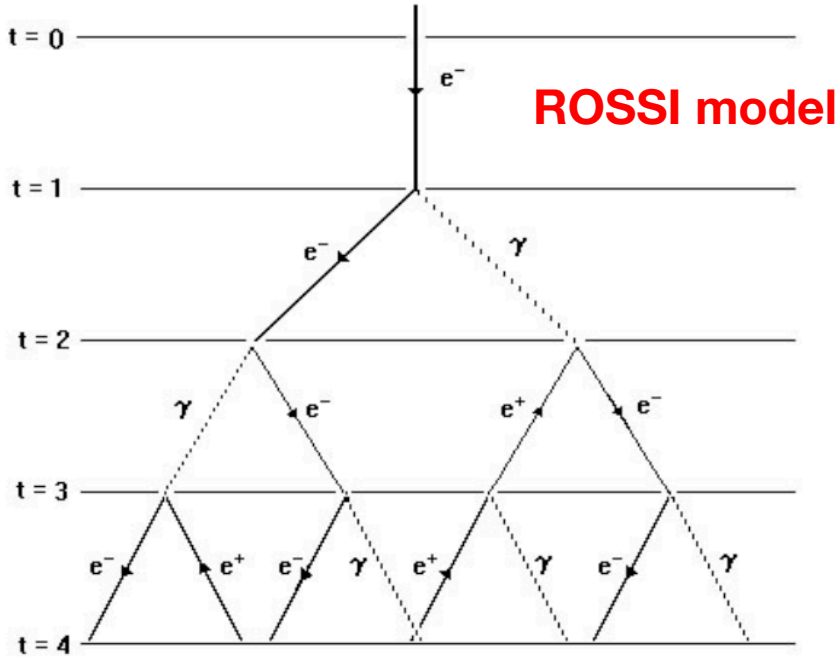

Il massimo dello sciame si ottiene ad $L_{max} = \ln (E_0/E_c) / \ln 2$
Lo sciame procede poi con processi dissipativi tipo ionizzazione, effetto Compton o fotoelettrico. Si forma così la coda dello sciame

Electromagnetic showers

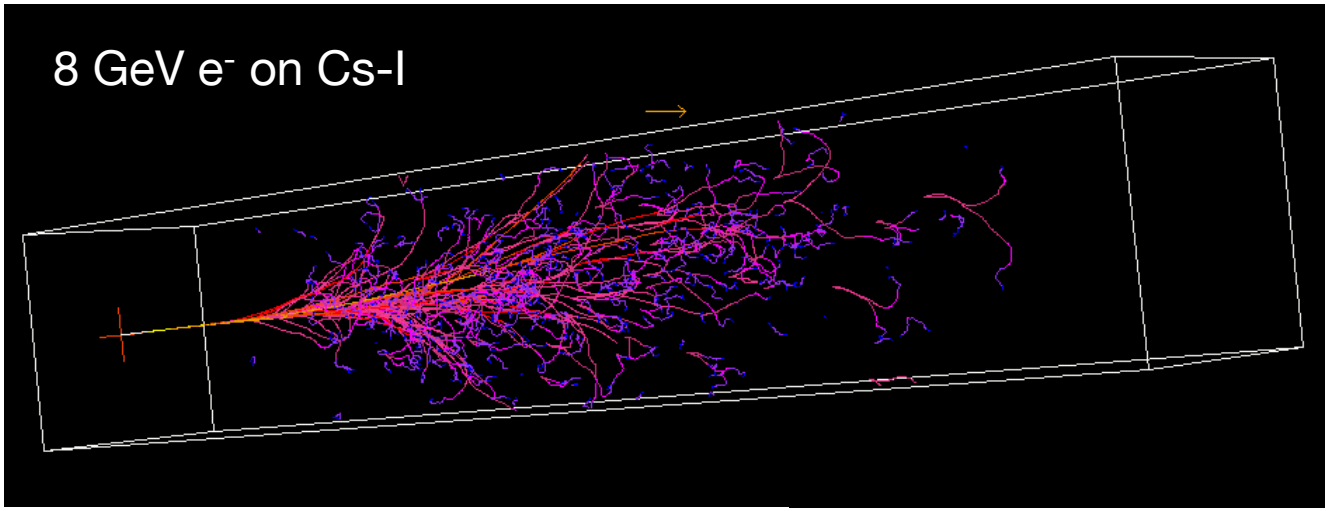

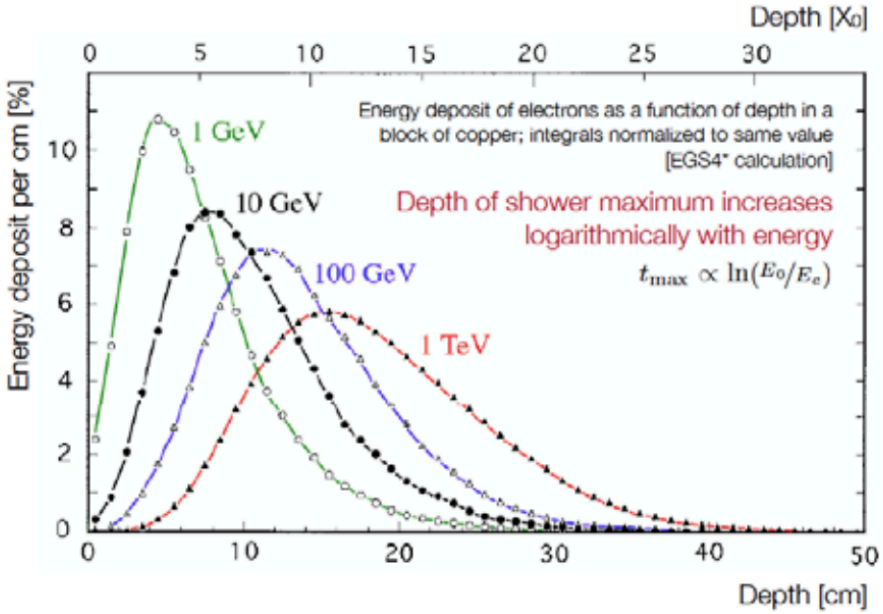

- Shower depth described by the material interaction length X_0
- **Increases logarithmically**
- At least 10 X_0 to absorb low energy showers

- Lateral width independent on energy. 95% of energy deposit contained in cylinder with **Molière radius**

$$R_M = 21\,\mathrm{MeV} \cdot X_0 / E_C$$

Electromagnetic showers

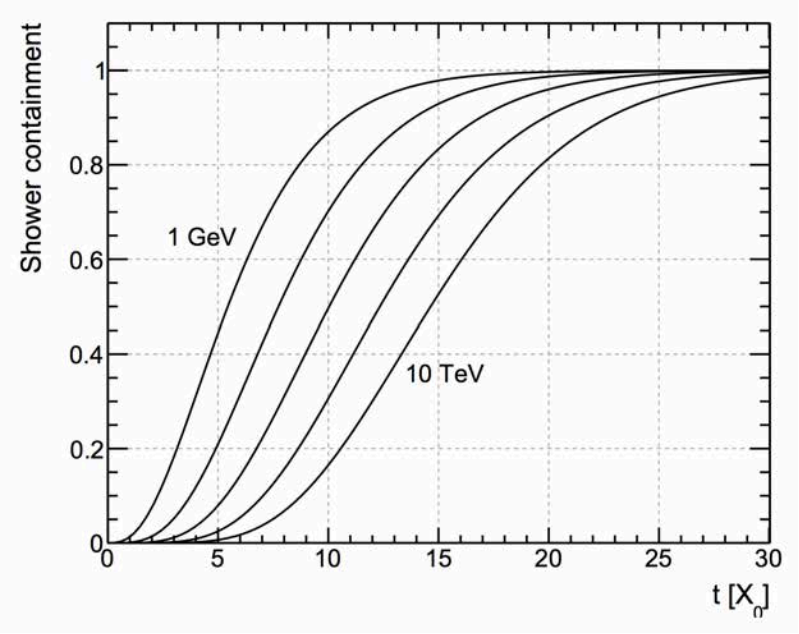

Material	X_0 [g cm^{-2}]	ϱ [g cm^{-3}]	X_0 [cm]
Pb	6.37	11.350	0.561
BGO	7.97	7.130	1.12
CsI	8.39	4.510	1.86
W	6.76	19.3	0.350
C (graphite)	42.70	2.210	19.3
Si	21.82	2.329	9.37
Air	36.62	1.2×10^{-3}	30,500

Space calorimeters must be compact and thick (in terms of X_0)

Two solutions:

- Homogeneous calorimeters (BGO, PWO, ….)
- Sampling calorimeters: passive material + active materials. Energy is sampled only in the active layers (silicon, gas, fibers, …)

Electromagnetic showers

Calorimetro a 'sandwich' scintillatore/piombo

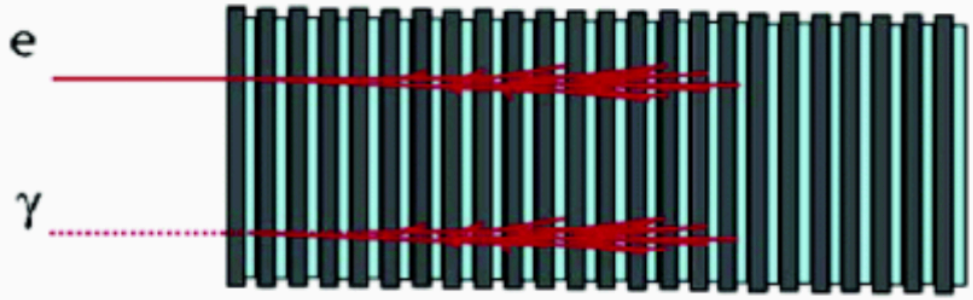

$\sigma E/E \sim 20\%/\sqrt{E}$

Calorimetro a cristalli omogenei

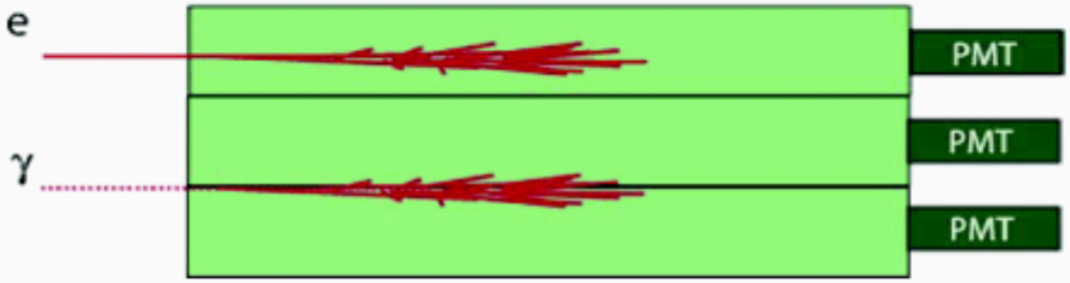

$\sigma E/E \sim 1\%/\sqrt{E}$

la misura di energia è un processo **distruttivo:**
dopo la misura calorimetrica la particella iniziale non esiste più

Electromagnetic showers

Energy resolution of a calorimeter can be parametrised as

$$\frac{\sigma(E)}{E} = \frac{a}{\sqrt{E}} \oplus \frac{b}{E} \oplus c$$

$\oplus$ means quadratic sum

- **a** the **stocastic term** accounts for any kind of Poisson-like fluctuations
  - natural merit of homogeneous calorimeters
  - several contributions add to the "intrinsic one"
- **b** the **noise term** responsible for degradation of low energy resolution
  - mainly the energy equivalent of the electronic noise
  - contribution from pileup: the fluctuation of energy entering the measurement area from sources other than the primary particle
- **c** the **constant term** dominates at high energy
  - its relevance is strictly connected to the small value of a
  - it is mostly dominated by the stability of calibration
  - contributions from energy leakage, non uniformity of signal generation and/or collection, loss of energy in dead materials,…

Calorimetry

I calorimetri si suddividono ulteriormente in:

- Calorimetri omogenei:
  - Rivelatore = assorbitore
  - Buona risoluzione in energia (~ 1-2%)
  - Risoluzione spaziale limitata nella direzione longitudinale
  - Usati solo per calorimetria e.m.
  - alto costo e danneggiabili dalle radiazioni

- Calorimetri a campionamento:
  - Rivelatore ed assorbitore separati → solo parte dell'energia viene misurata
  - Risoluzione in energia limitata
  - Buona risoluzione spaziale nella direzione longitudinale
  - Usati sia per calorimetria adronica che e.m.

Calorimetry

Calorimeters

Simple electromagnetic shower profile

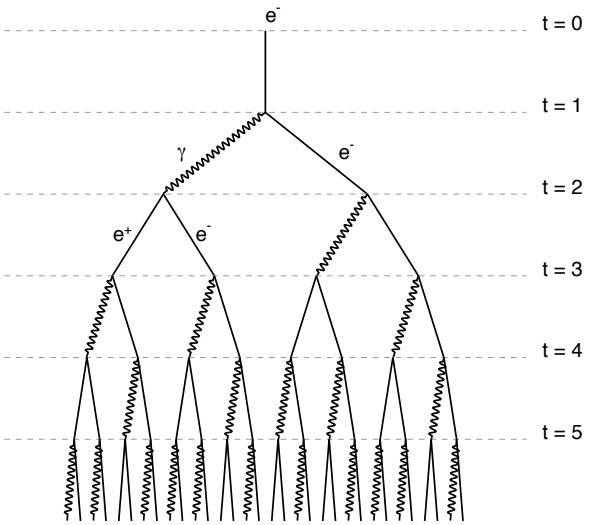

- Calorimeters measures the energy releases of the particle
  - Homogeneous / Sampling
  - Electromagnetic / Hadronic

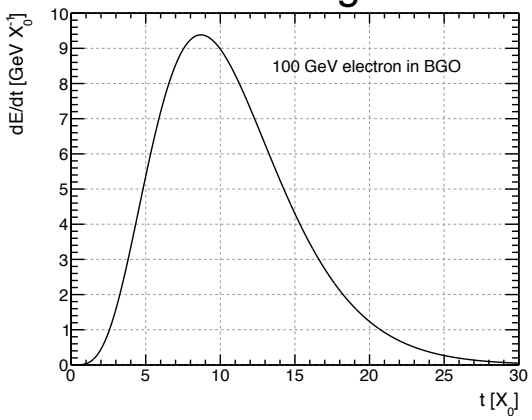

$$\frac{dE}{dt} = E_0 b \frac{(bt)^{a-1} e^{-bt}}{\Gamma(a)}$$

- The energy resolution improves as the energy increases

Statistical fluctuations

Inhomogenities, calibration, energy leaks,…

$$\frac{\sigma_E}{E} = \frac{a}{\sqrt{E}} \oplus \frac{b}{E} \oplus c$$

Electronics

- BUT: energy resolution is not everything. Tipically the dominant systematic is the knowledge of the energy scale!!
  - Resolution → Symmetric smearing of measured energy
  - Energy scale → Systematic shift of measured energy

Energy measurements

Magnetic Spectrometers

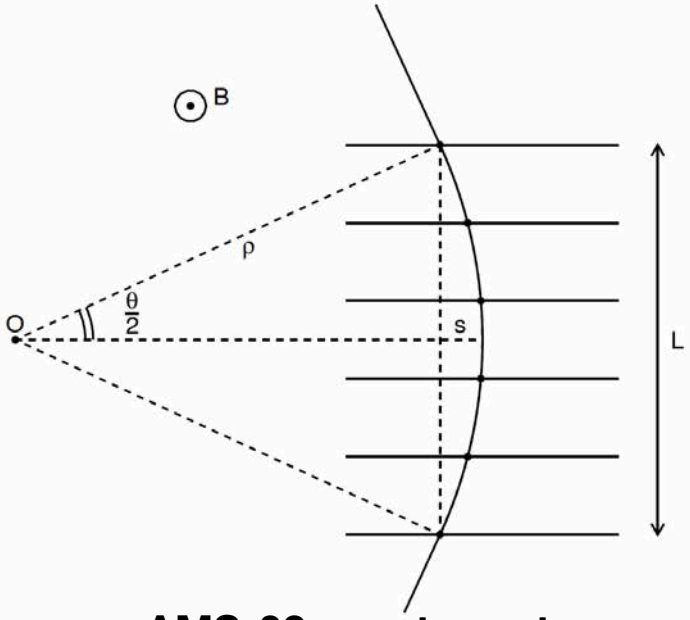

AMS-02 spectrometer

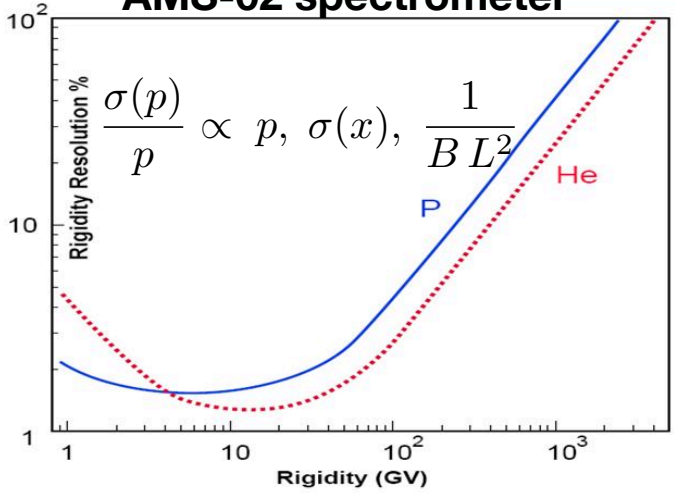

Calorimeters

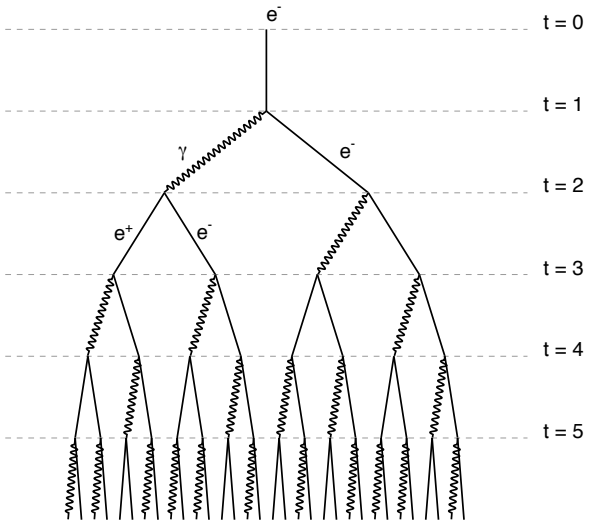

AMS-02 electromagnetic calorimeter

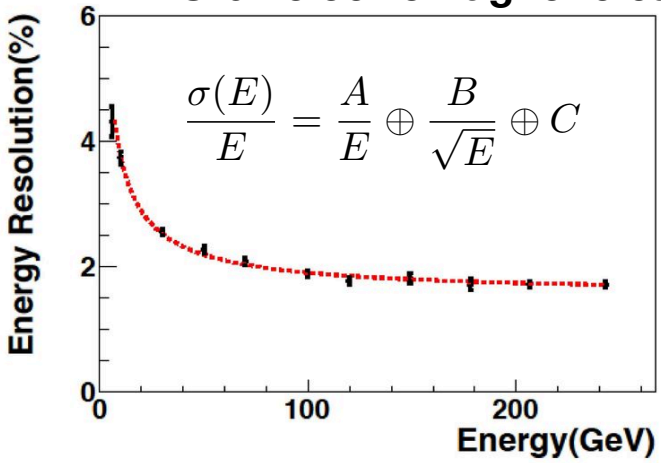

Instrument Acceptance

ACCEPTANCE: measurement of the collection capabilities of the detector

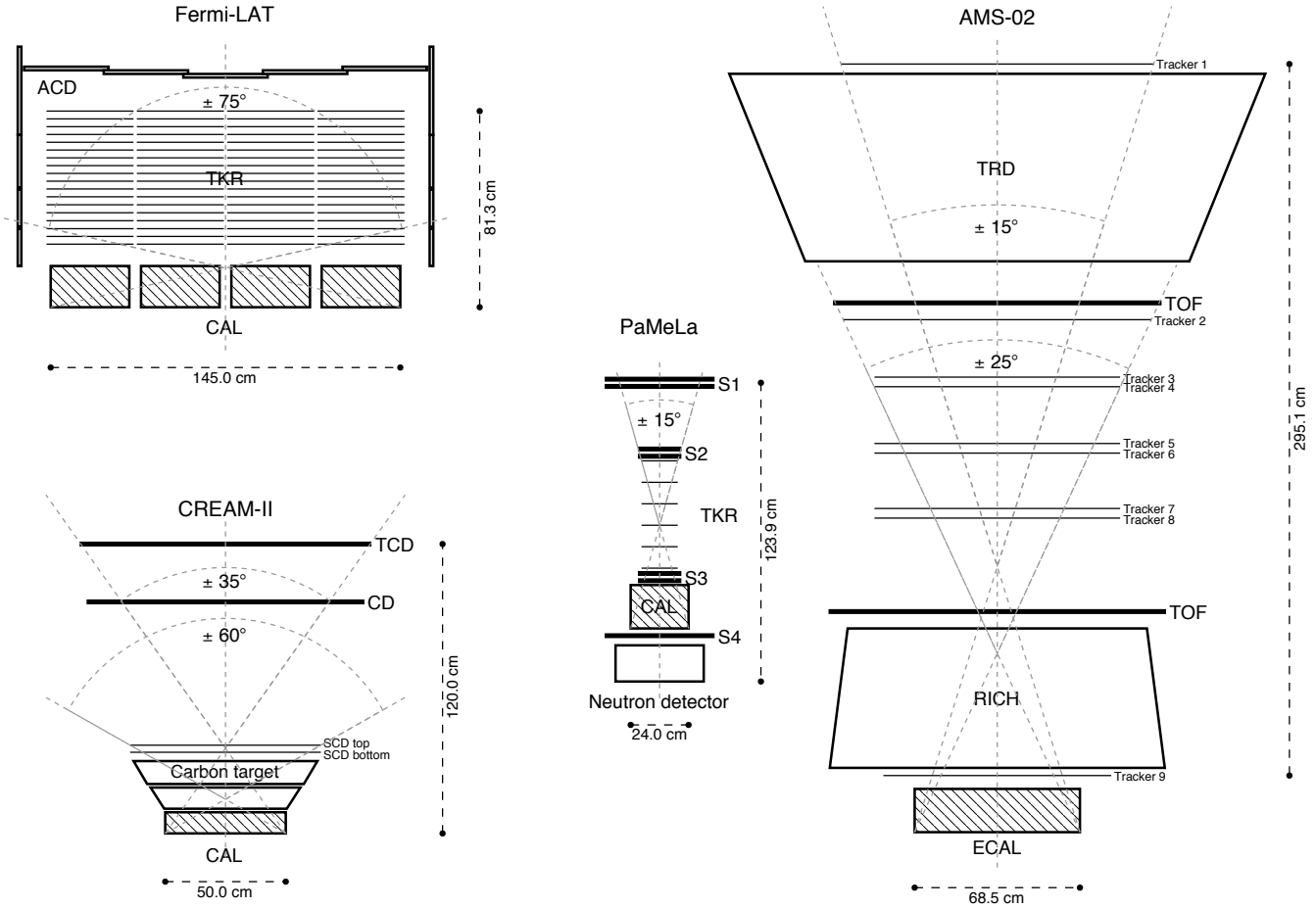

The more elongated is the detector, the less solid angle it can accept

Instrument Acceptance

ACCEPTANCE: measurement of the collection capabilities of the detector

The acceptance (or geometric factor) is formally defined as the integral of the effective area over the solid angle:

$$G(E) = \int_{\Omega} A_{\rm eff}(E, \theta, \phi) d\Omega, \qquad (77)$$

and the field of view as the ratio between the geometric factor and the effective area at normal incidence:

$$\mathrm{FoV}(E) = \frac{G(E)}{A_{\rm eff}^{\perp}(E)} = \frac{\int_{\Omega} A_{\rm eff}(E, \theta, \phi) d\Omega}{A_{\rm eff}^{\perp}(E)}. \qquad (78)$$

(Note that when the angular dependence of the effective area is different at different energies, the field of view does depend on energy, see, e.g., [78].)

A simple planar detector

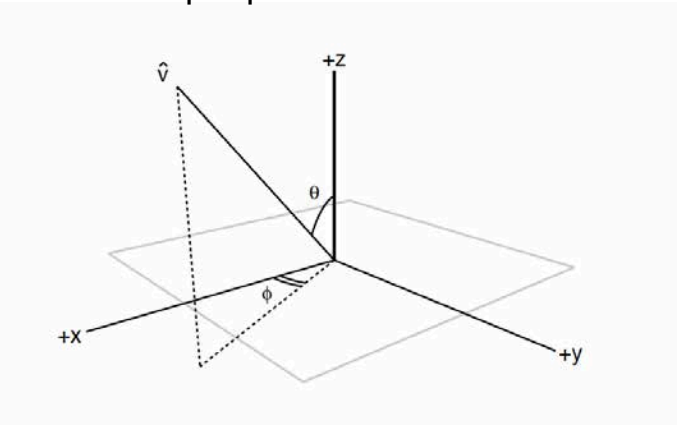

In this case the effective area at normal incidence is simply the geometrical area of the detector $S = l^2$. It is clear that $A_{\rm eff}$ only depends on the polar angle θ:

$$A_{\rm eff}(E, \theta, \phi) = S \cos\theta, \qquad (79)$$

and the acceptance reads:

$$G = S \int_0^{2\pi} d\phi \int_0^{\pi} \cos\theta \sin\theta d\theta = \pi S. \qquad (80)$$

The field of view, finally, is

$$\mathrm{FoV} = \frac{G}{S} = \pi. \qquad (81)$$

Instrument Acceptance

ACCEPTANCE: measurement of the collection capabilities of the detector
Tipically measured with MonteCarlo simulations including the detector geometry, materials and interactions with the detector

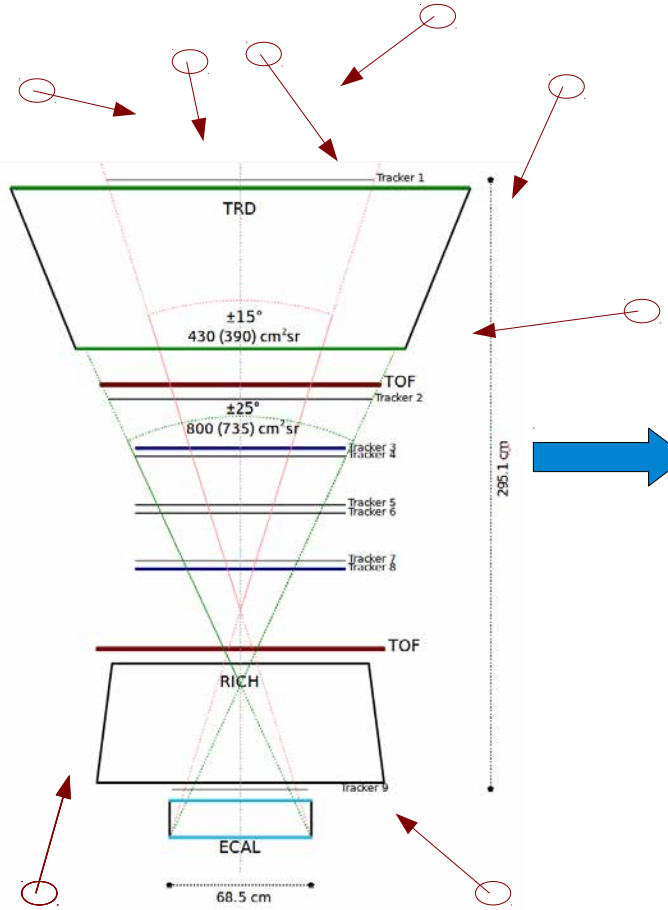

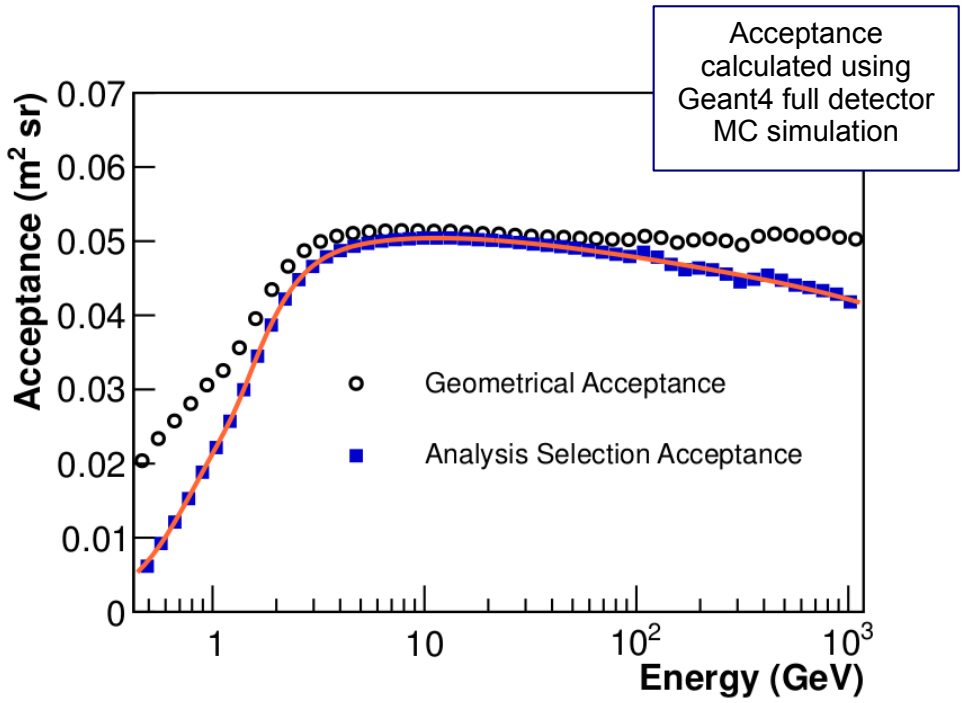

Instrument Gathering Power

GATHERING POWER: measurement of the collection capabilities of the mission (it includes the detector lifetime)

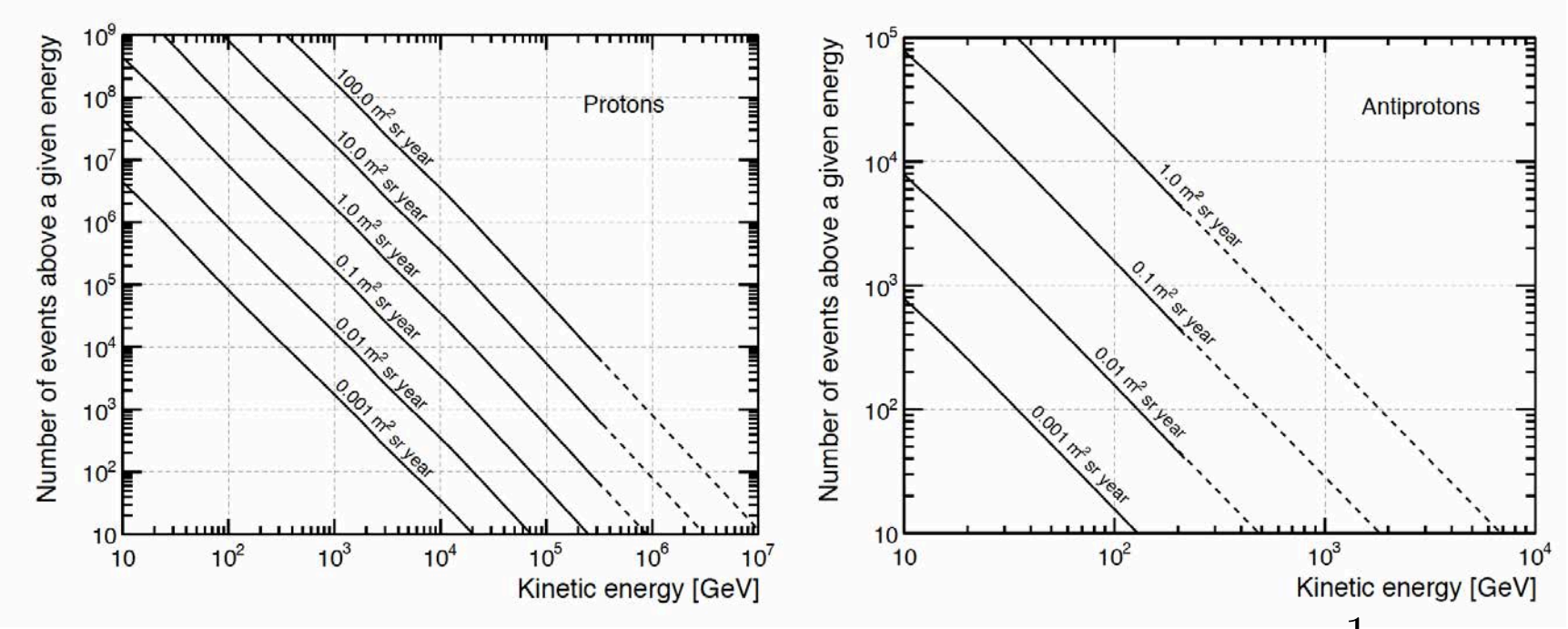

Statistical Error on Flux measurement $\propto \frac{1}{\sqrt{N}}$

Maximize Statistics < -- > Minimize statistical uncertainties

- Large acceptances
- Long duration missions

Typical quantities

- Cosmic ray physics is (almost) all about **FLUXES**

- **DIFFERENTIAL FLUX**: number of CRs per unit of time and energy (*) crossing the unit vector area towards a given direction in the sky
  - Measured in [$GeV^{-1}\ m^{-2}\ s^{-1}$]
  - Used for point source studies (like gamma rays)

- **FLUX or INTENSITY**: number of CRs per unit of time, energy (*) and solid angle crossing the unit vector area
  - Measured in [$GeV^{-1}\ m^{-2}\ s^{-1}\ sr^{-1}$]
  - Used for isotropic measurements (charged cosmic rays)

(*) Fluxes can be expressed as function of different improper definition of “energy”
  - Kinetik energy (calorimeters)
  - Kinetik energy per nucleon (calorimeters)
  - Rigidity (spectrometers)

Typical quantities

$$E_{\rm k} = E - mc^2$$

Kinetik Energy: defined by the acceleration due to electrostratic fields at the sources. Measured with calorimeters

$$\mathcal{E}_{\rm k} = \frac{E_{\rm k}}{A}$$

Kinetik Energy per Nucleon: defined by the spallation processes during propagation in the ISM medium. Quantity conserved in spallation processes. Measured with calorimeters (and hypothesis on the isotope composition)

$$R = \frac{pc}{Ze}$$

Rigidity: defines the motion in magnetic fields (for example, during diffusion through turbolent fields or curvature in homogeneuos fields). Measured with spectrometers

E	Energy	$[\mathrm{GeV}]$
$E_{\rm k}$	Kinetic energy	$[\mathrm{GeV}]$
$\mathcal{E}_{\rm k}$	Kinetic energy/nucleon	$[\mathrm{GeV}/A]$
p	Momentum	$[\mathrm{GeV/c}]$
R	Rigidity	$[\mathrm{GV}]$

Typical quantities

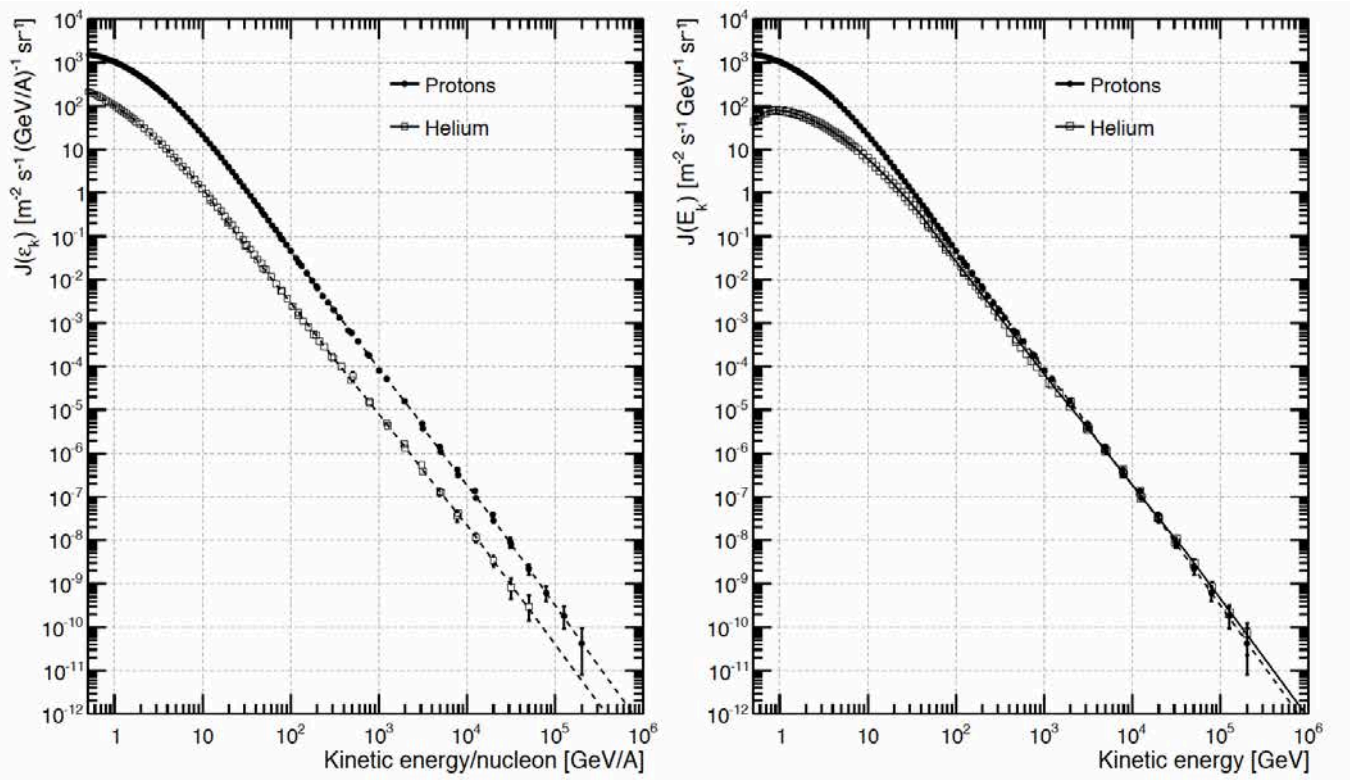

FIG. 2: Differential intensities, plotted as a function of kinetic energy per nucleon (left) and total kinetic energy (right) for the two most abundant CR species: protons and He nuclei. While the He intensity is a factor of ~ 10 smaller than that of protons at, say, ~ 1 TeV/nucleon, the two are comparable, at ~ 1 TeV, when binned in total kinetic energy. See next section for more

Beware: Fluxes are differential quantities (see units). Transformations from different unit on the X axis require the use of the Jacobian on the Y axis

The Flux Measurement

Precision knowledge of the detector acceptance, response and resolution, and of the data acquisition in space.

FLUX

Number of cosmic rays collected

$$\Phi(E) = \frac{N}{\Delta E \, \Delta T \, Acc \, \varepsilon_{sel} \, \varepsilon_{trig}}$$

Trigger Efficiency

Acceptance (m^2 sr)
usually calculated using MC sims

Energy/Rigidity (GeV)
size of the bin

Exposure Time (s)
also called "Livetime"

Particle selection efficiency
based on the statistical techniques employed to extract N

Each factor uncertainty contributes equally to the final measurement.
Systematic uncertainty studies for each factor are fundamental

Future experiments

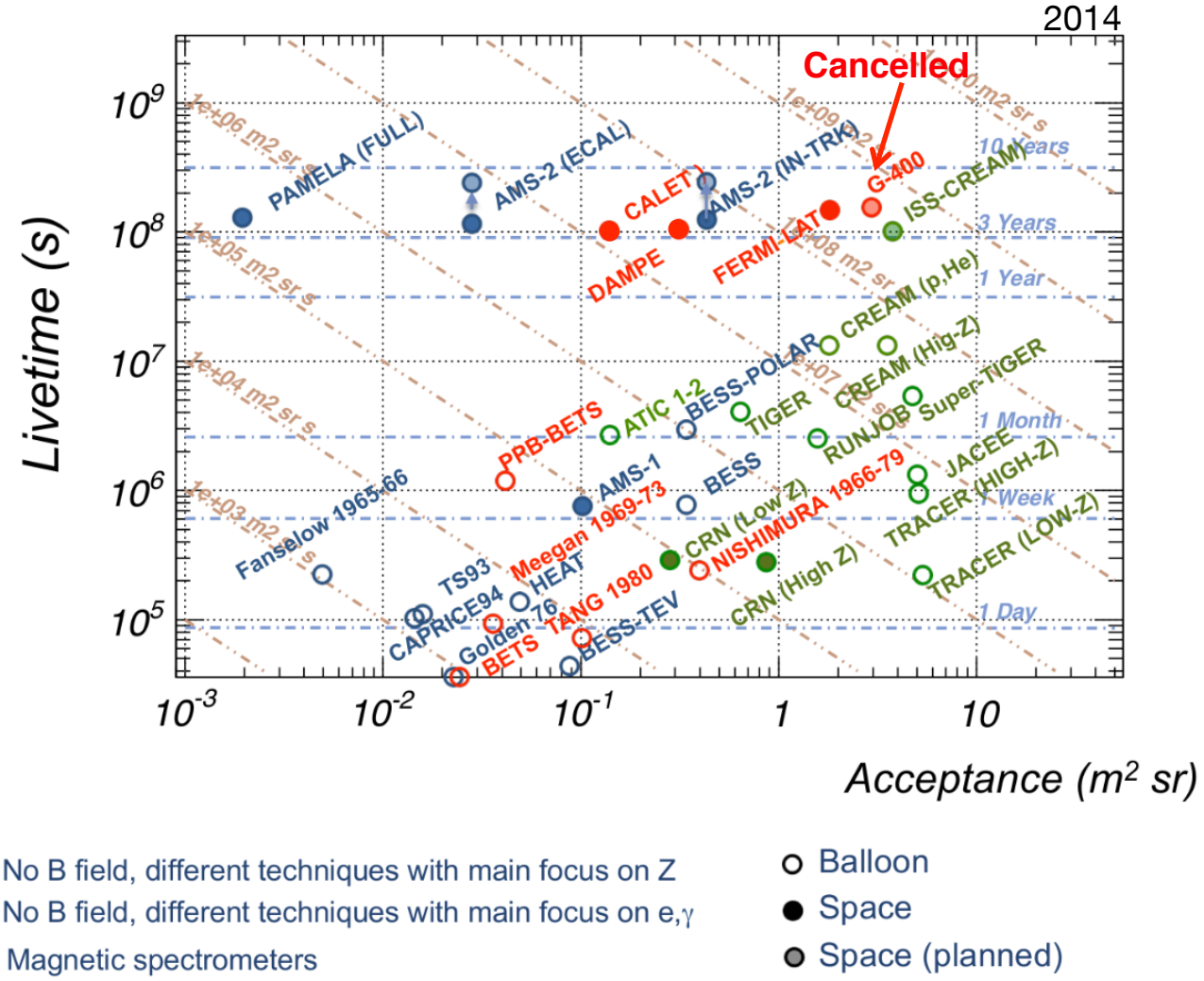

AMS-02 will be the unique magnetic spectrometer in space able to distinguish matter from antimatter for the next 10 years.